IEEE Access
Multidisciplinary ⋮ Rapid Review ⋮ Open Access Journal

Received 14 April 2025, accepted 3 May 2025, date of publication 6 May 2025, date of current version 22 May 2025.
Digital Object Identifier 10.1109/ACCESS.2025.3567561

RESEARCH ARTICLE

Advancing Smart Sensor Networks and Carbon-Based Biosensors Through Artificial Intelligence: A Deep Learning Approach to Optoelectronic Device Innovation

KELIANG LUO
Software Engineering Department, Faculty of Computer Science and Information Technology, Universiti Putra Malaysia, Kuala Lumpur 43400, Malaysia
e-mail: keliangluo2025@163.com

ABSTRACT This research proposes a novel artificial decision-marking framework suitable for modern smart sensor networks and carbon-based biosensor systems which deals with uncertainty and the peculiarity of the data. To achieve the goals, the approach relies on the optoelectronic properties of carbon nanomaterials and already combines AI and deep learning. This raises the level of sensing, real-time data fusion, and adaptive decision-making within the environment to unprecedented levels. To enhance sensor evaluation in sensor manufacturing, we take a step further and implement Dombi Interval Valued Intuitionistic Fuzzy Sets (D-IVIFs) and work with Dombi Interval Valued Intuitionistic Fuzzy Dombi Bonferroni Mean (D-IVIFDBM) for hierarchical decision-making. Moreover, two Multi-Attribute Group Decision Making (MAGDM) methods IVIFWDBM and IVIFWDGBM are developed for expert evaluation aggregation in selection tasks of different criteria to enhance selection accuracy. These experiments did demonstrate improvements in decision accuracy as well as better overall performance than conventional models of comparison. The numerical experiments showed that these methods are more effective than traditional MAGDM models. Introducing such an advanced decision framework in deep learning systems enables improved adaptability, security, and resilience in next-generation sensor networks and biosensor devices. The new paradigm enables real-time signal interpretation and adaptive learning and provides effective solutions in harsh environments where severe fluctuations are common. This study assists in addressing the discrepancy between conceptual decision models and actual physical achievements in smart sensing, which will foster the development of more sophisticated and efficient optoelectronic devices.

INDEX TERMS Modern smart sensor networks, biosensor systems based on carbon materials, hybrid neural-fuzzy systems with deep learning; Dombi operations, innovations in optoelectronic devices and artificial intelligence, systems of uncertainty modeling.

I. INTRODUCTION

The integration of artificial intelligence (AI) with smart sensor networks and carbon-based biosensors has emerged as a transformative approach in modern optoelectronic device innovation. With advancements in deep learning algorithms, sensor networks are evolving to become more efficient, adaptive, and capable of real-time decision-making. Carbon-based biosensors, due to their exceptional electrical, mechanical, and biocompatible properties, offer significant potential for applications in healthcare, environmental monitoring, and industrial automation. However, optimizing their performance and integrating them into scalable smart systems requires innovative computational approaches. AI, particularly deep learning, has demonstrated remarkable capabilities in data processing, pattern recognition, and predictive

The associate editor coordinating the review of this manuscript and approving it for publication was Mauro Fadda.

TABLE 1. Summary of the proposed hybrid framework for advancing optoelectronic device innovation.

Components	Descriptions
Deep Neural Network (DNN) Feature Extractor	Uses CNNs/RNNs to extract latent representations from the raw sensor and biosensor data
complex Circular Intuitionistic Fuzzy Sets (C-CIFS)	Models sensor uncertainty with circular membership functions and intuitionistic measures
Dombi Weighted Average Operator (C-CIFDWA)	Aggregates fuzzy information using a Dombi-based weighted average approach
Dombi Weighted Geometric Operator (C-CIFDWG)	Aggregates fuzzy data via a geometric weighting scheme based on Dombi operators
Hybrid Fuzzy–Deep Learning Framework	Integrates deep feature extraction with fuzzy aggregation (using both Dombi operators) to handle uncertain data Improved decision accuracy; dynamic adaptation to noise

analysis. When applied to sensor networks, AI enhances signal processing, improves detection sensitivity, and enables adaptive responses to complete environmental stimuli. In the context of carbon-based biosensors, deep learning algorithms facilitate real-time interpretation of biochemical signals, improving diagnostic accuracy and reliability. Furthermore, the integration of AI-driven analytics with optoelectronic devices enables the development of intelligent sensing systems that can operate autonomously, reducing human intervention and enhancing efficiency.

In the age of digital revolution, smart sensor networks and carbon-based biosensors are emerging as the key elements of applications ranging from healthcare diagnostics and environmental monitoring to industrial automation. Though increasingly more important, available decision-making models tend to disappoint when dealing with uncertainty, vagueness of data, and disagreement among experts' estimates. These shortcomings hamper the quality of intelligent sensing systems, particularly in complex and real-time domains. Moreover, the absence of integration between fuzzy decision models and sophisticated learning algorithms inhibits the creation of adaptive, high-performance optoelectronic devices. This underlines the necessity for a stronger, more intelligent decision-making paradigm that can efficiently address these challenges.

This study explores the convergence of AI, smart sensor networks, and carbon-based biosensors to advance optoelectronic device innovation. It examines how deep learning techniques can enhance sensor data interpretation, optimize biosensor performance, and drive advancements in smart sensing applications. By leveraging AI-driven methodologies, this research aims to address key challenges in sensor integration, data processing, and real-time decision-making, paving the way for the new generation of intelligent sensing technologies. The significant unpredictability of real-world settings makes it difficult to describe attribute values for alternatives in today's decision-making scenarios. Even though Zadeh's [1] 1965 invention of fuzzy sets (FSs) offered a useful tool for managing MAGDM and multi-attribute decision-making (MADM) problems, FSs' restriction to membership functions (MF) alone occasionally proves inadequate for capturing complete fuzzy information. When Atanassov [2] developed intuitionistic fuzzy sets (IFSs) in 1986, he presented a more complete framework that included an MF, a non-membership function (NMF), and an indeterminacy degree. With the inclusion of NMF and indeterminacy degrees, IFSs offer a more nuanced depiction of uncertainty than typical FSs, which solely take MF into account.

This makes it possible to handle ambiguous and imprecise information in decision-making processes using a more expressive and adaptable framework. Decision support systems, expert systems, pattern recognition, and decision analysis are just a few of the domains where IFSs are used. In situations where human judgment and subjective reasoning are important, they offer a useful tool for modeling and reasoning with ambiguous and partial data. This development made it easier to depict subtle, hazy elements, like scenarios with differing levels of agreement and resistance to voting results.

Atanassov and Gargov [3] developed the IFS further, describing the basic IVIFS approach and introducing the concept of IVIFS. An expansion of conventional IFSs, IVIFSs provide a more adaptable framework for capturing ambiguity and uncertainty in decision-making. In contrast to traditional IFSs, which provide each element in the discourse universe a specific MF, NMF, and indeterminacy degree, IVIFSs enable the encoding of fuzzy information as intervals. This means that IVIFSs allow for greater ambiguity and vagueness in decision-making scenarios by providing ranges or intervals within which MF, NMF, and indeterminacy degrees may lie rather than precise numbers. IVIFSs are used in many domains, such as MADM, where they help decision-makers make more solid and knowledgeable choices in the face of ambiguity by providing a more accurate depiction of imprecise data. By using IVIFSs, decision-makers may effectively negotiate ambiguity and uncertainty and gain a more thorough grasp of complicated decision settings. Relevant theories are applied to solve multi-attribute decision-making (MADM) challenges, including investment evaluation, pattern recognition, machine learning, and fundamentals planning [4], [5], [6], [7].

Recent developments in neural network-based computational models have proven highly promising for the solution of intricate nonlinear models, especially those with singularities, delays, and fractional dynamics. Various studies have established robust solvers based on neural networks, wavelet functions, and heuristic methods for a range of applications. For example, neural network methods have been successfully implemented in pantograph differential models [8], language learning systems [9], and hepatitis B virus dynamics [10]. Morlet and Meyer wavelet-based neural computation processes have been utilized for delay differential models, transport networks, and predator-prey interactions [11], [12], [13], [14]. Further works have considered functional nonlinear singular differential equations through Meyer wavelets [15], in addition to heuristic designs for modeling biological and medical systems like the modeling of smoking behavior and SITR COVID-19 models [16], [17], [18], [19]. Higher-order neuro-swarm hybrid methods, fractional-order and time-delay-based Lane–Emden equations and Emden–Fowler differential models have also been investigated to enhance the accuracy and stability of solutions in intricate systems [20], [21], [22], [23], [24]. Additionally, stochastic mathematical models have been constructed for epidemic management, such as coronavirus spread models [25]. These earlier contributions form necessary computational bases and prompt the incorporation of intelligent algorithms—like D-IVIF and deep learning—into sensor-based decision-making platforms.

The theory of IFSs has advanced significantly in recent years, with several accomplishments ranging from inventing aggregation operators (AOs) that are suited to the complexity of decision-making processes to conducting operations on IFSs. Extended AOs that can handle fuzzy information have recently been introduced, whereas classic AOs were only able to aggregate absolute values into a single real value. Choquet, power, dependent, prioritized, and density AOs are a few examples of these. For the aggregation of information, several types of aggregation operators (AOs) exist, but very few or none of them interrelate the input information. They play a significant role in processing various kinds of information used in decision-making, pattern identification, information retrieval, medical diagnosis, data mining, machine learning, etc. Over the past few decades, both scholars and researchers have been paying more attention to the study of AO [26], [27], [28], [29]. Power AO [30] is a widely used tool that considers the relationship of the information using some power weights. Another AO is the density AO proposed by Liu and Yu [31], which uses the attributes' density weights to find the input arguments' interrelationships. Bonferroni [32] introduced the notion of BMO, a mean-type aggregation operator used to consider the relationship of the aggregated information effectively. BM's most essential characteristic is that it captures the relationships between the combined arguments. Yager [33] initially improved and expanded the modeling capabilities of BM by substituting various mean-type operators for simple averaging. The BMO is a generalized form of the Heronian mean operator (HMO) proposed by Sykora [34]. Because of the effective behavior of BMO, this concept has been utilized in many fuzzy frameworks. The idea of BMOs in the setting of IFSs was comprehensively studied by Xu and Yager [35], and duplets of information were used to express the BMOs.

The Bonferroni mean (BM) operator is the most prominent progress, developed by Bonferroni [32] in 1950, to deal with intuitionistic fuzzy values (IFVs). Further, the concept of BMOs in the setting of IFSs was comprehensively studied by Xu and Yager [35], who proposed a few generalizations to improve their analytical ability. Many extensions were applied to the BMO. The concept of the geometric BM (GBM) operator was investigated by Xia et al. [36] and Li et al. [37]. The hesitant fuzzy BM (HFBM) operator was created by Zhu and Xu [38]. The HF geometric BM (HFGBM) operator was introduced by Zhu et al. [39]. The IFG power BM (IFGPBM) operator was developed by He et al. [40] by combining the GBM operator and the PM operator. The uncertain linguistic BM operators were presented by Wei et al. [41]. The intuitionistic uncertain linguistic partitioned BM operators were defined by Liu and Liu [42].

Dombi operations cannot be used to process the BM operator, even though it efficiently captures the relationships between parameters. Integrating the BM operator with Dombi operations to handle IFNs is necessary due to the growing requirement for more thorough processing of fuzzy information, especially in MAGDM situations. In 1982, Dombi [43] presented the Dombi t-norm and t-conorm, which meet the general requirements of t-norms and t-conorms. Using a parameter, the Dombi t-norm and t-conorm can generate a customizable aggregation technique. Many other authors used the Dombi t-norm and t-conorm in a variety of areas due to their importance [44], [45], and [46].

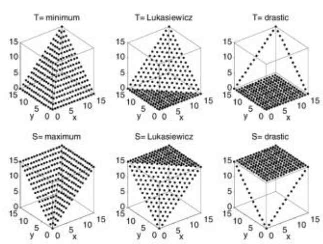

FIGURE 1. Representation of basics T norms and Conorms.

A. GOALS AND INSPIRATION

The rapid advancement of smart sensor networks and carbon-based biosensors has revolutionized numerous fields, including healthcare, environmental monitoring, and industrial automation. However, the challenge of processing and integrating uncertain, imprecise, and ambiguous sensor data remains a critical issue. This study proposes a novel approach by incorporating Dombi Aggregation Operators (AO) and BM within the Interval-Valued Intuitionistic Fuzzy Dombi Bonferroni Mean (IVIFDBM) framework to enhance decision-making in sensor-based systems. A key objective of this study is to optimize the integration of AI-driven deep learning techniques in sensor networks to improve data aggregation, processing, and interpretation. Carbon-based biosensors, known for their high sensitivity and biocompatibility, often face challenges in handling ambiguous and uncertain data from complete biological and environmental systems. The proposed IVIFDBM operators provide a robust mathematical framework to integrate these uncertain data streams, ensuring more accurate and reliable decision-making. This study demonstrates how deep learning algorithms, combined with advanced fuzzy aggregation techniques, can refine sensor data processing, thereby enhancing the accuracy, reliability, and adaptability of smart sensor networks and optoelectronic biosensing devices.

To validate the proposed methodologies, a hypothetical case study is presented, illustrating the practical applicability of IVIFDBM operators in real-world sensor-based decision-making scenarios. Additionally, two MAGDM approaches, utilizing IVIFWDBM and IVIFWDGBM operators, are introduced and tested on real-world datasets to verify their effectiveness in handling uncertain sensor information. By integrating these advanced fuzzy aggregation techniques with AI-powered deep learning approaches, this research aims to enhance optoelectronic device innovation, improve biosensor performance, and advance smart sensor network capabilities. The findings of this study will provide valuable insights into developing next-generation intelligent sensing technologies, capable of making autonomous, high-precision decisions in complete and uncertain environments.

B. MOTIVATION FOR THE STUDY

The increasing need for intelligent sensing technologies across healthcare diagnostics, environmental monitoring, and industrial automation has fueled the demand for accurate and flexible decision-making models. Such applications function in dynamic systems where data are incomplete, imprecise, or inconsistent. Conventional models are not capable of handling such uncertainties and are generally unable to respond in real time. Thus, developing sophisticated frameworks capable of handling ambiguous and interval-valued information, as well as facilitating timely and trustworthy decisions is crucial. Such a gap has been filled with this study in proposing a novel model integrating fuzzy logic with deep learning to extend decision-making capacities in smart sensors and biosensor systems.

1) EXISTING MODELS AND GAPS

Different models of fuzzy logic e.g., classical FSs, IFSs, PFSs, and IVIFSs have been extensively used throughout the years to interpret and analyze sensor readings. These models present adjustable mechanisms for handling vagueness and partial truth in uncertain decision-making situations. Yet they fail too often in practice when being applied to situations of extensive multidimensional uncertainty and conflicting analyses from several different experts. Most traditional solutions have static assumptions and do not have the dynamism required by real-time situations in dynamic environments.

2) NOVELTY AND CONTRIBUTIONS

To address these shortcomings, this research introduces a new MAGDM approach based on D-IVIFs. The Dombi operations have greater flexibility in representing the interaction between attributes and expert opinions so that uncertain information can be more accurately aggregated. In addition, the incorporation of deep learning methods brings intelligent feature extraction and adaptive learning features, allowing the system to adaptively respond to evolving input patterns. This combination not only enhances the decision-making process but also helps in the innovation of optoelectronic devices with enhanced precision and responsiveness.

C. THE PAPER IS ORGANIZED AS

1) INTRODUCTION

This section gives a general overview of manufacturing organizations' difficulties when choosing suppliers because of the ambiguity and uncertainty involved in weighing several factors. It also presents the suggested approach to solving this issue: Interval-Valued Intuitionistic Fuzzy Dombi Bonferroni Mean (IVIFDBM) operations.

2) LITERATURE REVIEW

This section examines relevant studies on fuzzy set theory, supplier selection techniques, and current methods for addressing ambiguity and uncertainty in decision-making processes. It provides the history and setting of the suggested IVIFDBM technique. The study explores the theoretical basis of IVIFDBM operators, elucidating their derivation from IVIFSs and their role in consolidating expert evaluations across different supplier evaluation criteria.

3) METHODOLOGY

The steps for using the IVIFDBM approach in supplier selection are described in this section. It explains how several factors, including dependability, competitive pricing, delivery time, and product quality, are considered and how to combine these evaluations using the IVIFDBM operators efficiently.

4) ILLUSTRATIVE CASE STUDY

A hypothetical case study is provided to show how to use the IVIFDBM approach in supplier selection. This case study demonstrates how the suggested method may be applied in practice and helps decision-makers find the best provider. Techniques for MAGDM: The paper presents two MAGDM approaches that use IVIFDBM operators.

In the last ten years, fuzzy logic has been applied to decision models to a great extent because it can handle uncertainty and vagueness in real-world systems. Zadeh's classic FSs formed the basis of imprecise data modeling but were limited by their failure to handle hesitation or dual membership. This drawback has motivated Atanassov to present IFSs which introduced a hesitation margin to capture uncertainty more appropriately. Then, IVIFSs are developed by extending this concept, making use of interval values for MF and NMF in making more flexible expert-driven evaluations.

Multiple scientists have implemented IVIFSs and their variants in MAGDM situations. For instance, Wang et al. used IVIF weighted aggregation operators in the optimization of a sensor network and Asif et al. utilized Pythagorean fuzzy aggregation strategies on environmental observations. Such models commonly lack dealing with interactions among factors or dynamic adaptability to adjusting aggregation action based on competing expertise.

Recent developments involve the application of q-rung orthopair fuzzy sets, neutrosophic sets, and picture fuzzy sets to enhance uncertainty modeling. However, these methods are inclined to add computational complexity without supporting flexible operator platforms. Additionally, the absence of contextual flexibility constrains their applicability in rapidly changing environments like smart sensor networks and intelligent biosensors.

To fill these voids, researchers have started incorporating fuzzy models with aggregation operators like BM, Hamacher, and Aczel-Alsina that enable the handling of interrelations between criteria. Yet, most models fail to leverage the complete potential of Dombi operations, which add a tunable parameter to manipulate the behavior of aggregation functions so that flexible decision fusion is facilitated.

At the same time, the advancement of deep learning has provided novel avenues for autonomous feature extraction and adaptive learning under rich data contexts. Deep learning, although previously examined in areas like image identification and predictive modeling, is mostly not explored under its fusion with fuzzy decision-making, especially concerning sensor networks as well as optoelectronic devices.

II. PRELIMINARIES

This part will present the Dombi t-conorm and t-norm, the BM operator, and the concept of IFS to make the issue easier to understand.

A. INTERVAL-VALUED INTUITIONISTIC FUZZY SETS

Classical FSs are generalized by IVIFSs. An IFS assigns an MF and NMF to each element, along with a hesitation value that represents the degree of ambiguity or uncertainty surrounding the element's membership status. IVIFSs expand on this concept by allowing the MF, NMF, and hesitation values to be intervals rather than exact values. To account for imprecision or uncertainty, we provide each element with a range of values rather than a single number. IVIFS is used in image processing, pattern recognition, decision-making, and other domains where managing and modeling ambiguity and uncertainty is essential. They provide a more expressive and adaptable framework than IFSs or traditional fuzzy sets with exact values for dealing with imprecise and uncertain data.

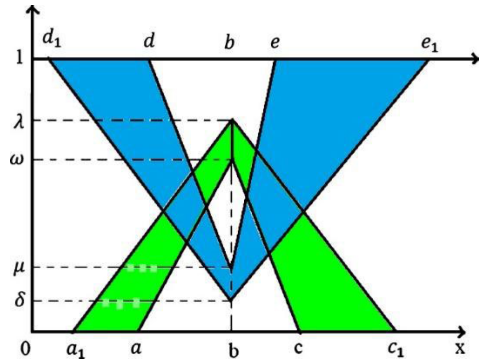

FIGURE 2. Graphical representation of interval-valued intuitionistic fuzzy set.

Definition 1 ([2]): An IFS Ƶin the universe of discourse Y is given by

$$\text{Ƶ}= \left\{ \begin{matrix} (<\mathcal{Y},\ (u_j(\mathcal{Y}),\ v_j(\mathcal{Y}))) \\ :\ 0 \leq\ \mu_B(\varkappa) +\ v_B(\varkappa) \leq 1\ \bar{a}nd\ \mathcal{Y} \in Y \end{matrix} \right\}$$

where $u_j(\mathcal{Y})$ is the MF, and $v_j(\mathcal{Y})$ is the NMF. For each point, $\mathcal{Y}$ in Y, and Y is a generic element. we have $u_j(\mathcal{Y}),\ v_j(\mathcal{Y}) \in [0,\ 1]$ and $0\ \leq\ u_j(\mathcal{Y}) +\ v_j(\mathcal{Y}) \leq 1$. For each IFS Ƶ in Y, let $\pi(\mathcal{Y})\ =\ 1-u_j(\mathcal{Y}) -\ v_j(\mathcal{Y}),\ \forall\ \mathcal{Y}\ \in\ Y$, and we call $\pi(\mathcal{Y})$ the indeterminacy degree of the element $\mathcal{Y}$ to the set Ƶ It can be easily proved that $0\ \leq\ \pi(\mathcal{Y}) \leq 1,\ \forall\ \mathcal{Y}\ \in\ Y$. To the given element $\mathcal{Y}$, the pair $(u_j(\mathcal{Y}),\ v_j(\mathcal{Y}))$ is called an intuitionistic fuzzy number (IFN). For convenience, we use $\bar{a}\ =\ (u_{\bar{a}},\ v_{\bar{a}})$ to represent IFN, which meets $u_{\bar{a}},\ v_{\bar{a}} \in [0,\ 1]$ and $0 \leq\ u_{\bar{a}} +\ v_{\bar{a}} \leq 1$.

Definition 2 ([47]): Let $\varrho_1 = ([u_1^l,\ u_1^u],\ [v_1^l,\ v_1^u]), \varrho_2 = ([u_2^l,\ u_2^u],\ [v_2^l,\ v_2^u])$ be two IVIFVs, then the operational laws that follow are stated.

1. $\varrho_1 \oplus \varrho_2 = (u_1^l +\ u_2^l - u_2^l u_2^l,\ v_1^l,\ v_2^l),$ $(u_1^u +\ u_2^u - u_2^u u_2^u,\ v_1^u,\ v_2^u)$
2. $\varrho_1 \otimes \varrho_2\ =\ (\ u_1^l u_2^l,\ \ v_1^l + v_2^l -\ \ v_1^l,\ v_2^l),\ (\ u_1^u u_2^u,\ \ v_1^u + v_2^u -\ \ v_1^u,\ v_2^u)$
3. $\zeta \varrho_1 = (1-(1-u_1^l)^\zeta,\ {v_1}^\zeta),\ (1-(1-u_1^u)^\zeta,\ {v_1}^\zeta),\ \zeta > 0$
4. ${\varrho_1}^\zeta = ({u_1}^\zeta, 1-(1-v_1^l)^\zeta), ({u_1}^\zeta, 1-(1-v_1^u)^\zeta)\ ,\ \zeta > 0$

Definition 3 ([47]): Let $\mathrm{a} = ([\mathrm{u}_\alpha^\mathrm{l},\ \mathrm{u}_\alpha^\mathrm{u}],\ [\mathrm{v}_\alpha^\mathrm{l},\ \mathrm{v}_\alpha^\mathrm{u}])$ be any IVIFN. Then, the Score Function is:

$$S(\varrho) = \frac{(u_\varrho^l)(1-v_\varrho^l) + (u_\varrho^u)(1-v_\varrho^u)}{2} \tag{1}$$

where $S(\varrho) \in [-1,\ 1]$.

B. THE BONFERRONI MEAN (BM) OPERATORS

In decision-making and multi-criteria decision analysis (MCDA), one kind of AO is the BM operator. They are a generalization of the weighted mean, quasi-arithmetic mean, and ordinary arithmetic mean operators, which were introduced by M. Grabisch and M. Roubens in 1995. By taking into account the size and degree of consistency of a set of numerical values, the BM operators aim to provide a comprehensive approach to merging them. When the input values show vague or unclear information, the BM operators are tolerant. The BM operators have several notable characteristics: Invariance of scale: When the input values are transformed in a positively linear fashion, the BM operator remains unchanged. Preserving order: The output of the BM operator will move in the same direction if all input values are changed simultaneously. Concordance: By giving higher weight to more concordant values, the BM operator shows the level of agreement between the input values. Different weighting coefficient selections can provide a variety of BM operators with distinctive traits and behaviors. For example, the weighted BM operator assigns extra weight to certain input values based on their perceived importance or dependability in the decision-making process. A flexible framework for merging vague or imprecise information is offered by the BM operators.

Definition 4 ([32]): If $\mathfrak{s}, \mathfrak{t} \geq 0$ and ϱ_i $(i = 1, 2, \ldots, \mathfrak{Y})$ are a set of real integers that are not negative, then the aggregation functions

$$BM^{\mathfrak{s},\mathfrak{t}}(\varrho_1, \varrho_2, \ldots, \varrho_{\mathfrak{Y}}) = \left(\frac{1}{\mathfrak{Y}(\mathfrak{Y}-1)} \sum_{\substack{i,j=1 \\ i \neq j}}^{\mathfrak{Y}} \varrho_i^{\mathfrak{s}} \varrho_j^{\mathfrak{t}}\right)^{\frac{1}{\mathfrak{s}+\mathfrak{t}}} \tag{2}$$

is called BM operator.

Definition 5 ([37]): If $\mathfrak{s}, \mathfrak{t} > 0$ and ϱ_i $(i = 1, 2, \ldots, \mathfrak{Y})$ are a set of real integers that are not negative, then the following is a description of the geometric Bonferroni mean (GBM) operator:

$$GBM^{\mathfrak{s},\mathfrak{t}}(\varrho_1, \varrho_2, \ldots, \varrho_{\mathfrak{Y}}) = \frac{1}{\mathfrak{s}+\mathfrak{t}} \left(\prod_{\substack{i,j=1 \\ i \neq j}}^{\mathfrak{Y}} (\mathfrak{s}\,\varrho_i + \mathfrak{t}\,\varrho_j)\right)^{\frac{1}{\mathfrak{Y}(\mathfrak{Y}-1)}} \tag{3}$$

C. DOMBI T-CONORM AND T-NORM

These operators were initially created in 1982 by Dombi [43], and extend standard logical conjunction and disjunction operators in fuzzy set theory (FS) by incorporating a flexible parameter that adjusts the aggregation process. The Dombi t-norm models intersection (AND operation) by smoothly combining membership values based on a control parameter ppp, ensuring adaptable strictness in fuzzy logic operations. Similarly, the Dombi t-conorm represents union (OR operation), allowing for a tunable disjunction of fuzzy values. These operators effectively handle uncertainty and vagueness, making them widely applicable in MADM, fuzzy logic control, pattern recognition, and artificial intelligence-based systems. Their ability to generalize standard norms makes them powerful tools for complex decision analysis and fuzzy aggregation methods.

Definition 6 ([43]): Consider two IFSs $A = \{< y, \varrho_A(y), \mathfrak{z}_A(y) > y \in Y\}$ and $B = \{< y, \varrho_B(y), \mathfrak{z}_B(y) > y \in Y\}$, we propose the generalized intersection and generalized union as follows:

$$A \cap_{\overline{T},\overline{T}^*} B = \{< y, \overline{T}(\varrho_A(y), \bar{a}_B(y)), \overline{T}^*(\mathfrak{z}_A(y), \mathfrak{z}_B(y)) > y \in Y\} \tag{4}$$

$$A \cup_{\overline{T},\overline{T}^*} B = \{< y, \overline{T}^*(\varrho_A(y), \bar{a}_B(y)), \overline{T}(\mathfrak{z}_A(y), \mathfrak{z}_B(y)) > y \in Y\} \tag{5}$$

where $\overline{T}$ signifies a T-norm and $\overline{T}^*$ denotes a T-conorm. Dombi (1982) suggested a generator to produce Dombi T-norm and T-conorm, which are given below.

$$\overline{T}_D(\mathfrak{m}, \mathfrak{n}) = \frac{1}{1+\left\{\left(\frac{1-\mathfrak{m}}{\mathfrak{m}}\right)^{\zeta} + \left(\frac{1-\mathfrak{n}}{\mathfrak{n}}\right)^{\zeta}\right\}^{\frac{1}{\zeta}}} \tag{6}$$

$$\overline{T}^{*\prime}_D(\mathfrak{m}, \mathfrak{n}) = 1 - \frac{1}{1+\left\{\left(\frac{\mathfrak{m}}{1-\mathfrak{m}}\right)^{\zeta} + \left(\frac{\mathfrak{n}}{1-\mathfrak{n}}\right)^{\zeta}\right\}^{\frac{1}{\zeta}}} \tag{7}$$

where $\zeta > 0$, $\mathfrak{m}, \mathfrak{n} \in [0, 1]$.

Based on the Dombi T-norm and T-conorm, we provide the following IVIFV operating rules:

Definition 7 ([47]): Suppose $\bar{a}_1 = ([\bar{a}_1^l, \bar{a}_1^u], [\mathfrak{z}_1^l, \mathfrak{z}_1^u])$ and $\bar{a}_2 = ([\bar{a}_2^l, \bar{a}_2^u], [\mathfrak{z}_2^l, \mathfrak{z}_2^u])$ are any two IVIFVs, then the operational laws of IVIFVs based on the Dombi T-norm and T-conorm can be defined as follows $(\zeta > 0)$, as shown in the equation at the bottom of the next page.

III. THE INTERVAL-VALUED INTUITIONISTIC FUZZY BONFERRONI MEAN OPERATORS BASED ON DOMBI T-NORM AND T-CONOR

In this section, based on the operational rules of IVIFVs from Dombi T-norm and T-conorm, we combine the BM about the proof of proposition 1. Please see Appendix I.

Definition 8: Consider $\bar{a}_i = ([\bar{a}_i^l, \bar{a}_i^u], [\mathfrak{z}_i^l, \mathfrak{z}_i^u])(i = 1, 2, \ldots, \mathfrak{Y})$ denote a set of IVIFVs, and $\mathfrak{s}, \mathfrak{t} \geq 0$, and IVIFDBM $: \Omega^{\mathfrak{Y}} \rightarrow \Omega$, if

$$IVIFDBM^{\mathfrak{s},\mathfrak{t}}(\varrho_1, \varrho_2, \ldots, \varrho_{\mathfrak{Y}}) = \left(\frac{1}{\mathfrak{Y}(\mathfrak{Y}-1)} \sum_{\substack{i,j=1 \\ i \neq j}}^{\mathfrak{Y}} \left(\bar{a}_i^{l\mathfrak{s}} \otimes_D \bar{a}_j^{l\mathfrak{t}}\right)\left(\bar{a}_i^{u\mathfrak{s}} \otimes_D \bar{a}_j^{u\mathfrak{t}}\right)\right)^{\frac{1}{\mathfrak{s}+\mathfrak{t}}} \tag{8}$$

When Ω is the collection of all IVIFVs, IVIFDBM is called the IVIFDBM operator. The aggregation results displayed in Proposition 1 can be obtained using the operational laws of the IVIFVs given in the calculations.

Proposition 1: Consider $\bar{a}_{i} = \left(\left[\bar{a}^{l}_{i},\ \bar{a}^{u}_{i}\right],\ \left[\mathfrak{z}^{l}_{i},\ \mathfrak{z}^{u}_{i}\right]\right)$ $\left(i = 1, 2, \ldots, \mathfrak{Y}\right)$ denote a set of IVIFVs, and $\mathfrak{s}, \mathfrak{b} \geq 0,\ \zeta > 0$, then the result aggregated is still an IVIFV, and even (9), as shown at the bottom of the next page.

We shall examine a few of the IVIFDBM operator's characteristics in the following sections.

Proposition 2 (Monotonicity): Consider $\left(\varrho'_1, \varrho'_2, \ldots, \varrho'_{\mathfrak{Y}}\right)$ and $\left(\varrho_1, \varrho_2, \ldots, \varrho_{\mathfrak{Y}}\right)$ are two sets of IVIFVs, if $\varrho'_{i} = \left(\varrho'_{i}, \mathfrak{z}'_{i}\right)$ and $\varrho_{i} = (\varrho_{i}, \mathfrak{z}_{i})$, $\varrho'_{i} \leq \varrho_{i}$, $\mathfrak{z}'_{i} \geq \mathfrak{z}_{i}$ for all $k = 1,\ 2,\ \ldots,\ \mathfrak{Y}$, then

$$IVIFDBM^{\mathfrak{s},\mathfrak{b}}\left(\varrho'_1, \varrho'_2, \ldots, \varrho'_{\mathfrak{Y}}\right) \leq IVIFDBM^{\mathfrak{s},\mathfrak{b}}\left(\varrho_1, \varrho_2, \ldots, \varrho_{\mathfrak{Y}}\right) \tag{10}$$

Proposition 3 (Idempotency): Let $\varrho_{i} = (\varrho_{i}, \mathfrak{z}_{i})$, $i = (1,\ 2,\ \ldots,\ \mathfrak{Y})$ denotes a set of the IVIFVs if all, $\varrho_{i}(i = 1,\ 2,\ \ldots,\ \mathfrak{Y})$ are equal, i.e., $\varrho_{i} = \varrho = (\bar{a},\ \mathfrak{z})$, $i = 1,\ 2,\ \ldots,\ \mathfrak{Y}$, then

$$IVIFDBM^{\mathfrak{s},\mathfrak{b}}\left(\varrho_1, \varrho_2, \ldots, \varrho_{\mathfrak{Y}}\right) = \varrho \tag{11}$$

Proposition 4 (Boundedness): Let $\varrho_{i} = \left(\varrho_{i}, \mathfrak{z}_{i}\right)$, $i = (1,\ 2,\ \ldots,\ \mathfrak{Y})$ denotes a set of IVIFVs, and $\bar{a}^{+} = \left(\underset{i=1}{\mathrm{ma\mathfrak{m}}}(\varrho_{i}),\ \underset{i=1}{\min}(\mathfrak{z}_{i})\right)$, $\bar{a}^{-} = \left(\underset{i=1}{\min}(\bar{a}_{i}),\ \underset{i=1}{\mathrm{ma\mathfrak{m}}}(\mathfrak{z}_{i})\right)$, then

$$\bar{a}^{-} \leq IVIFDBM\left(\varrho_1, \varrho_2, \ldots, \varrho_{\mathfrak{Y}}\right) \leq \bar{a}^{+} \tag{12}$$

Proof: See Appendix A.

Definition 9: Let $\bar{a}_{i} = \left(\left[\bar{a}^{l}_{i}, \bar{a}^{u}_{i}\right], \left[\mathfrak{z}^{l}_{i},\ \mathfrak{z}^{u}_{i}\right]\right)$ $\left(i = 1, 2, \ldots, \mathfrak{Y}\right)$ denotes a set of IVIFVs, and $\mathfrak{s}, \mathfrak{b} \geq 0,\ \zeta > 0$ and IVIFWDBM : $\Omega^{\mathfrak{Y}} \rightarrow \Omega$ if

$$IVIFWDBM^{\mathfrak{s},\mathfrak{b}}\left(\varrho_1, \varrho_2, \ldots, \varrho_{\mathfrak{Y}}\right) = \left(\frac{1}{\mathfrak{Y}\left(\mathfrak{Y}-1\right)} \sum_{\substack{i,j=1 \\ i \neq j}}^{\mathfrak{Y}} \frac{\left(w_{i}\bar{a}^{l\mathfrak{s}}_{i} \otimes_D w_j \bar{a}^{l\mathfrak{b}}_{j}\right)}{\left(w_{i}\bar{a}^{u\mathfrak{s}}_{i} \otimes_D w_j \bar{a}^{u\mathfrak{b}}_{j}\right)}\right)^{\frac{1}{\mathfrak{s}+\mathfrak{b}}} \tag{13}$$

$$1.\quad \bar{a}_1 \oplus \bar{a}_2 = \left(\left[\begin{array}{c} 1-\dfrac{1}{1+\left\{\left(\dfrac{a^{l}_1}{1-a^{l}_1}\right)^{\zeta}+\left(\dfrac{a^{l}_2}{1-a^{l}_2}\right)^{\zeta}\right\}^{\frac{1}{\zeta}}}, \\ 1-\dfrac{1}{1+\left\{\left(\dfrac{a^{u}_1}{1-a^{u}_1}\right)^{\zeta}+\left(\dfrac{a^{u}_2}{1-a^{u}_2}\right)^{\zeta}\right\}^{\frac{1}{\zeta}}} \end{array}\right],\ \left[\begin{array}{c} \dfrac{1}{1+\left\{\left(\dfrac{1-\mathfrak{z}^{l}_1}{\mathfrak{z}^{l}_1}\right)^{\zeta}+\left(\dfrac{1-\mathfrak{z}^{l}_2}{\mathfrak{z}^{l}_2}\right)^{\zeta}\right\}^{\frac{1}{\zeta}}}, \\ \dfrac{1}{1+\left\{\left(\dfrac{1-\mathfrak{z}^{u}_1}{\mathfrak{z}^{u}_1}\right)^{\zeta}+\left(\dfrac{1-\mathfrak{z}^{u}_2}{\mathfrak{z}^{u}_2}\right)^{\zeta}\right\}^{\frac{1}{\zeta}}} \end{array}\right]\right)$$

$$2.\quad \bar{a}_1 \otimes \bar{a}_2 = \left(\left[\begin{array}{c} \dfrac{1}{1+\left\{\left(\dfrac{1-\bar{a}^{l}_1}{a^{l}_1}\right)^{\zeta}+\left(\dfrac{1-a^{l}_2}{a^{l}_2}\right)^{\zeta}\right\}^{\frac{1}{\zeta}}}, \\ \dfrac{1}{1+\left\{\left(\dfrac{1-a^{u}_1}{a^{u}_1}\right)^{\zeta}+\left(\dfrac{1-a^{u}_2}{a^{u}_2}\right)^{\zeta}\right\}^{\frac{1}{\zeta}}} \end{array}\right],\ \left[\begin{array}{c} 1-\dfrac{1}{1+\left\{\left(\dfrac{\mathfrak{z}^{l}_1}{1-\mathfrak{z}^{l}_1}\right)^{\zeta}+\left(\dfrac{\mathfrak{z}^{l}_2}{1-\mathfrak{z}^{l}_2}\right)^{\zeta}\right\}^{\frac{1}{\zeta}}}, \\ 1-\dfrac{1}{1+\left\{\left(\dfrac{\mathfrak{z}^{u}_1}{1-\mathfrak{z}^{u}_1}\right)^{\zeta}+\left(\dfrac{\mathfrak{z}^{u}_2}{1-\mathfrak{z}^{u}_2}\right)^{\zeta}\right\}^{\frac{1}{\zeta}}} \end{array}\right]\right)$$

$$3.\ n\bar{a} = \left(\left[1-\frac{1}{1+\left\{n\left(\frac{a^{l}_1}{1-a^{l}_1}\right)^{\zeta}\right\}^{\frac{1}{\zeta}}},\ 1-\frac{1}{1+\left\{n\left(\frac{a^{u}_1}{1-a^{u}_1}\right)^{\zeta}\right\}^{\frac{1}{\zeta}}}\right],\ \left[\frac{1}{1+\left\{n\left(\frac{1-\mathfrak{z}^{l}_1}{\mathfrak{z}^{l}_1}\right)^{\zeta}\right\}^{\frac{1}{\zeta}}},\ \frac{1}{1+\left\{n\left(\frac{1-\mathfrak{z}^{u}_1}{\mathfrak{z}^{u}_1}\right)^{\zeta}\right\}^{\frac{1}{\zeta}}}\right]\right)$$

$$4.\ \bar{a}^{n} = \left(\left[\frac{1}{1+\left\{n\left(\frac{1-\mathfrak{z}^{l}_1}{\mathfrak{z}^{l}_1}\right)^{\zeta}\right\}^{\frac{1}{\zeta}}},\ \frac{1}{1+\left\{n\left(\frac{1-\mathfrak{z}^{u}_1}{\mathfrak{z}^{u}_1}\right)^{\zeta}\right\}^{\frac{1}{\zeta}}}\right],\ \left[1-\frac{1}{1+\left\{n\left(\frac{a^{l}_1}{1-a^{l}_1}\right)^{\zeta}\right\}^{\frac{1}{\zeta}}},\ 1-\frac{1}{1+\left\{n\left(\frac{a^{u}_1}{1-a^{u}_1}\right)^{\zeta}\right\}^{\frac{1}{\zeta}}}\right],\right)$$

where Ω is the set of all IVIFVs, and $w = (w_1, w_2, \ldots, w_{\mathfrak{Y}})^{\overline{T}}$ is the weight vector of $(\varrho_1, \varrho_2, \ldots, \varrho_{\mathfrak{Y}})$, $w_j \in [0,\ 1]$, $\sum_{j=1}^{\mathfrak{Y}} w_j = 1$*IVIFWDBM is* the IVIFWDBM operator.

Proposition 5: suppose $\bar{a}_i = \left(\left[\bar{a}_i^l,\ \bar{a}_i^u\right],\ \left[\mathfrak{z}_i^l,\ \mathfrak{z}_i^u\right]\right)$ $(i = 1, 2, \ldots, \mathfrak{Y})$ denotes a set of IVIFVs, and $\mathfrak{s},\ \mathfrak{b} \geq 0,\ \zeta > 0$, then the aggregated result is still on IVIFV, and even, as shown in the equation at the bottom of the next page.

Regarding the proof of Proposition 5, please see Appendix V. In the following section, we will explore some characteristics of the IVIFWDBM operator.

Proposition 6 (Monotonicity): Let $\left(\varrho_1', \varrho_2', \ldots, \varrho_{\mathfrak{Y}}'\right)$ and $(\varrho_1, \varrho_2, \ldots, \varrho_{\mathfrak{Y}})$ are two sets of IVIFVs, if $\varrho_i' = \left(\varrho'_i, \mathfrak{z}'_i\right)$ and $\varrho_i = (\varrho_i, \mathfrak{z}_i)$, $\varrho_i' \leq \varrho_i$, $\mathfrak{z}'_i \geq \mathfrak{z}_i$ for all $\tau = 1,\ 2,\ \ldots,\ \mathfrak{Y}$, then

$$\begin{aligned} &IVIFWDBM^{\mathfrak{s},\mathfrak{b}}\left(\varrho_1', \varrho_2', \ldots, \varrho_{\mathfrak{Y}}'\right) \\ &\quad \leq IVIFWDBM^{\mathfrak{s},\mathfrak{b}}\left(\varrho_1, \varrho_2, \ldots, \varrho_{\mathfrak{Y}}\right) \end{aligned} \tag{14}$$

Proposition 7 (Boundedness): Let $\varrho_i = \left(\varrho_i, \mathfrak{z}_i\right)$, $i = (1,\ 2,\ \ldots,\ \mathfrak{Y})$ denotes a set of IVIFVs, and $\bar{a}^+ = \left(\bar{a}^+_{m\bar{a}x},\ \mathfrak{z}^+{}_{min,}\right)$, $\bar{a}^- = \left(\bar{a}^-_{min,}\ \mathfrak{z}^-{}_{m\bar{a}x,}\right)$, $\zeta > 0$ where

$$\begin{aligned} \bar{a}^+_{m\bar{a}x} &= 1\Bigg/\left(1 + \left(\frac{\mathfrak{Y}(\mathfrak{Y}-1)}{\mathfrak{s}+\mathfrak{b}}\left(\frac{1-\max_{i=1}\left(\varrho_i\right)}{\max_{i=1}\left(\varrho_i\right)}\right)^{\zeta} \times 1\Bigg/\left(\sum_{\substack{i,j=1\\ i\neq j}}^{\mathfrak{Y}} 1\Bigg/\left(\frac{\mathfrak{s}}{w_i}+\frac{\mathfrak{b}}{w_j}\right)\right)\right)^{1/\zeta}\right)\mathfrak{z}^+{}_{\mathfrak{Y}in} \\ &= 1 - 1\Bigg/\left(\left(1+\frac{\mathfrak{Y}(\mathfrak{Y}-1)}{\mathfrak{s}+\mathfrak{b}} \times \left(\frac{\min_{i=1}\left(\mathfrak{z}_i\right)}{1-\min_{i=1}\left(\mathfrak{z}_i\right)}\right)^{\zeta} \Bigg/ \left(\sum_{\substack{i,j=1\\ i\neq j}}^{\mathfrak{Y}} 1\Bigg/\left(\frac{\mathfrak{s}}{w_i}+\frac{\mathfrak{b}}{w_j}\right)\right)\right)^{1/\zeta}\right) \\ \bar{a}^-_{\mathfrak{Y}in} &= 1 \end{aligned}$$

$$\begin{aligned} &IVIFDBM^{\mathfrak{s},\mathfrak{b}}\left(\varrho_1, \varrho_2, \ldots, \varrho_{\mathfrak{Y}}\right) \\ &= \left(1\Bigg/\left(\left(1+\frac{\mathfrak{Y}(\mathfrak{Y}-1)}{\mathfrak{s}+\mathfrak{b}} \times 1\Bigg/\left(\sum_{\substack{i,j=1\\ i\neq j}}^{\mathfrak{Y}} 1\Bigg/\left(\mathfrak{s}\left(\frac{1-\bar{a}_i^l}{\bar{a}_i^l}\right)^{\zeta} + \mathfrak{b}\left(\frac{1-\bar{a}_j^l}{\bar{a}_j^l}\right)^{\zeta}\right)\right)\right)^{1/\zeta}, \left(\frac{\mathfrak{Y}(\mathfrak{Y}-1)}{\mathfrak{s}+\mathfrak{b}} \times 1\Bigg/\left(\sum_{\substack{i,j=1\\ i\neq j}}^{\mathfrak{Y}} 1\Bigg/\left(\mathfrak{s}\left(\frac{1-\bar{a}_i^u}{\bar{a}_i^u}\right)^{\zeta} + \mathfrak{b}\left(\frac{1-\bar{a}_j^u}{\bar{a}_j^u}\right)^{\zeta}\right)\right)\right)^{1/\zeta}\right)\right), 1 - \right. \\ &\left. \left(1\Bigg/\left(1+\left(\times\frac{\frac{\mathfrak{Y}(\mathfrak{Y}-1)}{\mathfrak{s}+\mathfrak{b}}1}{\left(\sum_{\substack{i,j=1\\ i\neq j}}^{\mathfrak{Y}} 1\Bigg/\left(\mathfrak{s}\left(\frac{\mathfrak{z}_i^l}{1-\mathfrak{z}_1^l}\right)^{\zeta} + \mathfrak{b}\left(\frac{\mathfrak{z}_j^l}{1-\mathfrak{z}_j^l}\right)^{\zeta}\right)\right)}\right)^{1/\zeta}\right), \left(\frac{\mathfrak{Y}(\mathfrak{Y}-1)}{\mathfrak{s}+\mathfrak{b}} \times 1\Bigg/\left(\sum_{\substack{i,j=1\\ i\neq j}}^{\mathfrak{Y}} \frac{1}{\left(\mathfrak{s}\left(\frac{\mathfrak{z}_i^u}{1-\mathfrak{z}_1^u}\right)^{\zeta} + \mathfrak{b}\left(\frac{\mathfrak{z}_j^u}{1-\mathfrak{z}_j^u}\right)^{\zeta}\right)}\right)\right)^{1/\zeta}\right) \end{aligned} \tag{9}$$

$$/\left(1+\left(\frac{\mathfrak{Y}(\mathfrak{Y}-1)}{\mathfrak{s}+\mathfrak{b}}\left(\frac{1-\min\limits_{\mathrm{i}=1}\left(\varrho_{\mathrm{i}}\right)}{\min\limits_{\mathrm{i}=1}\left(\varrho_{\mathrm{i}}\right)}\right)^{\zeta}\times 1/\left(\sum_{\substack{\mathrm{i},j=1\\ \mathrm{i}\neq j}}^{\mathfrak{Y}}1/\left(\frac{\mathfrak{s}}{w_{\mathrm{i}}}+\frac{\mathfrak{b}}{w_j}\right)\right)\right)^{1/\zeta}\right)$$

$$\mathfrak{z}^{-}{}_{\mathfrak{Y}\bar{a}x}$$

$$=1-1/\left(1+\left(\frac{\mathfrak{Y}(\mathfrak{Y}-1)}{\mathfrak{s}+\mathfrak{b}}\times\left(\frac{\max\limits_{\mathrm{i}=1}\left(\mathfrak{z}_{\mathrm{i}}\right)}{1-\max\limits_{\mathrm{i}=1}\left(\mathfrak{z}_{\mathrm{i}}\right)}\right)^{\zeta}/\left(\sum_{\substack{\mathrm{i},j=1\\ \mathrm{i}\neq j}}^{\mathfrak{Y}}1/\left(\frac{\mathfrak{s}}{w_{\mathrm{i}}}+\frac{\mathfrak{b}}{w_j}\right)\right)\right)^{1/\zeta}\right)$$

Then

$$\bar{a}^{-}\leq IVIFWDBM\left(\varrho_1,\varrho_2,\ldots,\varrho_{\mathfrak{Y}}\right)\leq\bar{a}^{+}\tag{15}$$

In the following sections, we will examine a few geometric aggregation operators for IVIFVs based on Dombi operations.

Definition 10: Consider $\bar{a}_{\mathrm{i}}=\left(\left[\bar{a}^{l}_{\mathrm{i}},\ \bar{a}^{u}_{\mathrm{i}}\right],\ \left[\mathfrak{z}^{l}_{\mathrm{i}},\ \mathfrak{z}^{u}_{\mathrm{i}}\right]\right)$ $(\tau=1,2,\ldots,\mathfrak{Y})$ denotes a set of IVIFVs, and $\mathfrak{s},\mathfrak{b}\geq 0,\ \zeta>0$ and IVIFDGBM : $\Omega^{\mathfrak{Y}}\rightarrow\Omega$ if

$$IVIFDGBM^{\mathfrak{s},\mathfrak{b}}\left(\varrho_1,\varrho_2,\ldots,\varrho_{\mathfrak{Y}}\right)=\frac{1}{\mathfrak{s}+\mathfrak{b}}\prod_{\substack{\mathrm{i},j=1\\ \mathrm{i}\neq j}}^{\mathfrak{Y}}\left(\mathfrak{s}\varrho_{\mathrm{i}}\oplus_D\mathfrak{b}\varrho_j\right)^{\frac{1}{\mathfrak{Y}(\mathfrak{Y}-1)}}\tag{16}$$

When Ω represents the collection of all IVIFVs, IVIFDGBM is the interval-valued intuitionistic fuzzy Dombi geometric Bonferroni mean operator with fuzzy Dombi values.

Proposition 8: Let $\bar{a}_{\mathrm{i}}=\left(\left[\bar{a}^{l}_{\mathrm{i}},\ \bar{a}^{u}_{\mathrm{i}}\right],\ \left[\mathfrak{z}^{l}_{\mathrm{i}},\ \mathfrak{z}^{u}_{\mathrm{i}}\right]\right)$ $(\tau=1,2,\ldots,\mathfrak{Y})$ denotes a set of IVIFVs, and $\mathfrak{s},\mathfrak{b}\geq 0,\ \zeta>0$, then the result aggregated is still on IVIFV, and even (17), as shown at the bottom of the next page.

The proof, identical to Proposition 1's, is not included here.

Some features of the IVIFDGBM operator will be shown below.

Proposition 9 (Monotonicity): Suppose $\left(\varrho'_1,\varrho'_2,\ldots,\varrho'_{\mathfrak{Y}}\right)$ and $\left(\varrho_1,\varrho_2,\ldots,\varrho_{\mathfrak{Y}}\right)$ are two sets of IVIFVs, if $\varrho'_{\mathrm{i}}=\left(\varrho'_{\mathrm{i}},\mathfrak{z}'_{\mathrm{i}}\right)$ and $\varrho_{\mathrm{i}}=(\varrho_{\mathrm{i}},\mathfrak{z}_{\mathrm{i}})$, $\varrho'_{\mathrm{i}}\leq\varrho_{\mathrm{i}}$, $\mathfrak{z}'_{\mathrm{i}}\geq\mathfrak{z}_{\mathrm{i}}$ for all $\mathrm{i}=1,\ 2,\ \ldots,\ \mathfrak{Y}$, and $\mathfrak{s},\mathfrak{b}\geq 0,\ \zeta>0$ then

$$IVIFDGBM^{\mathfrak{s},\mathfrak{b}}\left(\varrho'_1,\varrho'_2,\ldots,\varrho'_{\mathfrak{Y}}\right)\leq IVIFDGBM^{\mathfrak{s},\mathfrak{b}}\left(\varrho_1,\varrho_2,\ldots,\varrho_{\mathfrak{Y}}\right)\tag{18}$$

The proof, identical to Proposition 2's, is not included here.

Proposition 10 (Idempotency): Let $\varrho_{\mathrm{i}}=(\varrho_{\mathrm{i}},\mathfrak{z}_{\mathrm{i}})$, $\mathrm{i}=(1,\ 2,\ \ldots,\ \mathfrak{Y})$ denotes a set of the IVIFVs if all,

$$IVIFWDBM^{\mathfrak{s},\mathfrak{b}}\left(\varrho_1,\varrho_2,\ldots,\varrho_{\mathfrak{Y}}\right)$$

$$=\left(\begin{array}{c}1/\left(\begin{array}{c}1+\left(\frac{\mathfrak{Y}(\mathfrak{Y}-1)}{\mathfrak{s}+\mathfrak{b}}\times 1/\left(\sum\limits_{\substack{\mathrm{i},j=1\\ \mathrm{i}\neq j}}^{\mathfrak{Y}}1/\left(\frac{\mathfrak{s}}{w_{\mathrm{i}}\left(\frac{\bar{a}^{l}_{\mathrm{i}}}{1-\bar{a}^{l}_{\mathrm{i}}}\right)^{\zeta}}+\frac{\mathfrak{b}}{w_j\left(\frac{\bar{a}^{l}_{j}}{1-\bar{a}^{l}_{j}}\right)^{\zeta}}\right)\right)\right)^{1/\zeta}\\ \left(\frac{\mathfrak{Y}(\mathfrak{Y}-1)}{\mathfrak{s}+\mathfrak{b}}\times 1/\left(\sum\limits_{\substack{\mathrm{i},j=1\\ \mathrm{i}\neq j}}^{\mathfrak{Y}}1/\left(\frac{\mathfrak{s}}{w_{\mathrm{i}}\left(\frac{\bar{a}^{u}_{\mathrm{i}}}{1-\bar{a}^{u}_{\mathrm{i}}}\right)^{\zeta}}+\frac{\mathfrak{b}}{w_j\left(\frac{\bar{a}^{u}_{j}}{1-\bar{a}^{u}_{j}}\right)^{\zeta}}\right)\right)\right)^{1/\zeta}\end{array}\right)\end{array},\ 1-\left(\begin{array}{c}\frac{1}{\left(1+\left(\frac{\mathfrak{Y}(\mathfrak{Y}-1)}{\mathfrak{s}+\mathfrak{b}}\times 1/\left(\sum_{\substack{\mathrm{i},j=1\\ \mathrm{i}\neq j}}^{\mathfrak{Y}}1/\left(\frac{\mathfrak{s}}{w_{\mathrm{i}}\left(\frac{1-\mathfrak{z}^{l}_{\mathrm{i}}}{\mathfrak{z}^{l}_{\mathrm{i}}}\right)^{\zeta}}+\frac{\mathfrak{b}}{w_j\left(\frac{1-\mathfrak{z}^{l}_{j}}{\mathfrak{z}^{l}_{j}}\right)}\right)\right)\right)^{1/\zeta}\right)},\\ \left(\frac{\mathfrak{Y}(\mathfrak{Y}-1)}{\mathfrak{s}+\mathfrak{b}}\times 1/\left(\sum\limits_{\substack{\mathrm{i},j=1\\ \mathrm{i}\neq j}}^{\mathfrak{Y}}1/\left(\frac{\mathfrak{s}}{w_{\mathrm{i}}\left(\frac{1-\mathfrak{z}^{u}_{\mathrm{i}}}{\mathfrak{z}^{u}_{\mathrm{i}}}\right)^{\zeta}}+\frac{\mathfrak{b}}{w_j\left(\frac{1-\mathfrak{z}^{u}_{j}}{\mathfrak{z}^{u}_{j}}\right)}\right)\right)\right)^{1/\zeta}\end{array}\right)\right)$$

$\varrho_{\mathsf{i}} (\mathsf{i} = 1, 2, \ldots, \mathfrak{Y})$ are equal, i.e., $\varrho_{\mathsf{i}} = \varrho = (\bar{a}, \mathfrak{z})$, $\mathsf{i} = 1, 2, \ldots, \mathfrak{Y}$, and $\mathfrak{s}, \mathfrak{t} \geq 0$, $\zeta > 0$ then

$$IVIFDGBM^{\mathfrak{s},\mathfrak{t}} (\varrho_1, \varrho_2, \ldots, \varrho_{\mathfrak{Y}}) = \varrho \tag{19}$$

The proof, identical to Proposition 3's, is not included here.

Proposition 11 (Boundedness): Let $\varrho_{\mathsf{i}} = \left(\varrho_{\mathsf{i}}, \mathfrak{z}_{\mathsf{i}}\right)$, $\mathsf{i} = (1, 2, \ldots, \mathfrak{Y})$ denotes a set of IVIFVs, and $\bar{a}^{+} = \left(\max_{\mathsf{i}=1}(\varrho_{\mathsf{i}}), \min_{\mathsf{i}=1}(\mathfrak{z}_{\mathsf{i}})\right)$, $\bar{a}^{-} = \left(\min_{\mathsf{i}=1}(\bar{a}_{\mathsf{i}}), \max_{\mathsf{i}=1}(\mathfrak{z}_{\mathsf{i}})\right)$, and $\mathfrak{s}, \mathfrak{t} \geq 0$, $\zeta > 0$ then

$$\bar{a}^{-} \leq IVIFDGBM (\varrho_1, \varrho_2, \ldots, \varrho_{\mathfrak{Y}}) \leq \bar{a}^{+} \tag{20}$$

Proof: Please See Appendix B.

Definition 11: Suppose $\bar{a}_{\mathsf{i}} = \left(\left[\bar{a}^l_{\mathsf{i}}, \bar{a}^u_{\mathsf{i}}\right], \left[\mathfrak{z}^l_{\mathsf{i}}, \mathfrak{z}^u_{\mathsf{i}}\right]\right)$ $(\mathsf{i} = 1, 2, \ldots, \mathfrak{Y})$ denotes a set of IVIFVs, and $\mathfrak{s}, \mathfrak{t} \geq 0$, $\zeta > 0$ and IVIFWDGBM : $\Omega^{\mathfrak{Y}} \to \Omega$ if

$$IVIFWDGBM^{\mathfrak{s},\mathfrak{t}} (\varrho_1, \varrho_2, \ldots, \varrho_{\mathfrak{Y}})$$
$$= \frac{1}{\mathfrak{s}+\mathfrak{t}} \prod_{\substack{\mathsf{i},j=1 \\ \mathsf{i}\neq j}}^{\mathfrak{Y}} \left(\mathfrak{s}\left(\varrho_{\mathsf{i}}\right)^{w_{\mathsf{i}}} \oplus_D \mathfrak{t}(\varrho_j)^{w_j}\right)^{\frac{1}{\mathfrak{Y}(\mathfrak{Y}-1)}} \tag{21}$$

When Ω represents the collection of all IVIFVs, the operator IVIFWDGBM is called the interval-valued intuitionistic fuzzy weighted Dombi geometric Bonferroni mean (IVIFWDGBM).

Proposition 12: Let $\bar{a}_{\mathsf{i}} = \left(\left[\bar{a}^l_{\mathsf{i}}, \bar{a}^u_{\mathsf{i}}\right], \left[\mathfrak{z}^l_{\mathsf{i}}, \mathfrak{z}^u_{\mathsf{i}}\right]\right)$ $(\mathsf{i} = 1, 2, \ldots, \mathfrak{Y})$ denotes a set of IVIFVs, and $\mathfrak{s}, \mathfrak{t} \geq 0$, $\zeta > 0$, then the result aggregated is still on IVIFN, and even (22), as shown at the bottom of the next page.

Proposition 13 (Monotonicity): Suppose $(\varrho'_1, \varrho'_2, \ldots, \varrho'_{\mathfrak{Y}})$ and $(\varrho_1, \varrho_2, \ldots, \varrho_{\mathfrak{Y}})$ are two sets of IVIFVs, if $\varrho'_{\mathsf{i}} = \left(\varrho'_{\mathsf{i}}, \mathfrak{z}'_{\mathsf{i}}\right)$ and $\varrho_{\mathsf{i}} = (\varrho_{\mathsf{i}}, \mathfrak{z}_{\mathsf{i}})$, $\varrho'_{\mathsf{i}} \leq \varrho_{\mathsf{i}}$, $\mathfrak{z}'_{\mathsf{i}} \geq \mathfrak{z}_{\mathsf{i}}$ for all $\mathsf{i} = 1, 2, \ldots, \mathfrak{Y}$, and $\mathfrak{s}, \mathfrak{t} \geq 0$, $\zeta > 0$ then

$$IVIFWDGBM^{\mathfrak{s},\mathfrak{t}} \left(\varrho'_1, \varrho'_2, \ldots, \varrho'_{\mathfrak{Y}}\right) \leq IVIFWDGBM^{\mathfrak{s},\mathfrak{t}} (\varrho_1, \varrho_2, \ldots, \varrho_{\mathfrak{Y}}) \tag{23}$$

$$IVIFDGBM^{\mathfrak{s},\mathfrak{t}} (\varrho_1, \varrho_2, \ldots, \varrho_{\mathfrak{Y}})$$
$$= \left(\left(1 - \frac{1}{1 + \left(\frac{\mathfrak{Y}(\mathfrak{Y}-1)}{\mathfrak{s}+\mathfrak{t}} \times \frac{1}{\sum_{\substack{\mathsf{i},j=1\\ \mathsf{i}\neq j}}^{\mathfrak{Y}} \frac{1}{\left(\mathfrak{s}\left(\frac{\bar{a}^l_{\mathsf{i}}}{1-\bar{a}^l_{\mathsf{i}}}\right)^{\zeta} + \mathfrak{t}\left(\frac{\bar{a}^l_j}{1-\bar{a}^l_j}\right)^{\zeta}\right)}} \right)^{1/\zeta}}, \left(\frac{\mathfrak{Y}(\mathfrak{Y}-1)}{\mathfrak{s}+\mathfrak{t}} \times \frac{1}{\sum_{\substack{\mathsf{i},j=1\\ \mathsf{i}\neq j}}^{\mathfrak{Y}} \frac{1}{\left(\mathfrak{s}\left(\frac{\bar{a}^u_{\mathsf{i}}}{1-\bar{a}^u_{\mathsf{i}}}\right)^{\zeta} + \mathfrak{t}\left(\frac{\bar{a}^u_j}{1-\bar{a}^u_j}\right)^{\zeta}\right)}} \right)^{1/\zeta} \right), \left(\frac{1}{1 + \left(\frac{\mathfrak{Y}(\mathfrak{Y}-1)}{\mathfrak{s}+\mathfrak{t}} \times \frac{1}{\sum_{\substack{\mathsf{i},j=1\\ \mathsf{i}\neq j}}^{\mathfrak{Y}} \frac{1}{\left(\mathfrak{s}\left(\frac{1-\mathfrak{z}^l_{\mathsf{i}}}{\mathfrak{z}^l_1}\right)^{\zeta} + \mathfrak{t}\left(\frac{1-\mathfrak{z}^l_j}{\mathfrak{z}^l_j}\right)^{\zeta}\right)}} \right)^{1/\zeta}}, \left(\frac{\mathfrak{Y}(\mathfrak{Y}-1)}{\mathfrak{s}+\mathfrak{t}} \times \frac{1}{\sum_{\substack{\mathsf{i},j=1\\ \mathsf{i}\neq j}}^{\mathfrak{Y}} \frac{1}{\left(\mathfrak{s}\left(\frac{1-\mathfrak{z}^u_{\mathsf{i}}}{\mathfrak{z}^u_1}\right)^{\zeta} + \mathfrak{t}\left(\frac{1-\mathfrak{z}^u_j}{\mathfrak{z}^u_j}\right)^{\zeta}\right)}} \right)^{1/\zeta} \right) \right) \tag{17}$$

Proposition 14 (Idempotency): Let $\varrho_{\imath} = (\varrho_{\imath}, \mathfrak{z}_{\imath})$, $\imath = (1, 2, \ldots, \mathfrak{Y})$ denotes a set of the IVIFVs if all, $\varrho_{\imath} (\imath = 1, 2, \ldots, \mathfrak{Y})$ are equal, i.e., $\varrho_{\imath} = \varrho = (\bar{a}, \mathfrak{z})$, $\imath = 1, 2, \ldots, \mathfrak{Y}$, and $\mathfrak{s}, \mathfrak{b} \geq 0$, $\zeta > 0$ then

$$IVIFWDGBM^{\mathfrak{s},\mathfrak{b}} (\varrho_1, \varrho_2, \ldots, \varrho_{\mathfrak{Y}}) = \varrho \tag{24}$$

Proposition 15 (Boundedness): Let $\varrho_{\imath} = \left(\varrho_{\imath}, \mathfrak{z}_{\imath}\right)$, $\imath = (1, 2, \ldots, \mathfrak{Y})$ denote a set of IVIFVs, and $\bar{a}^{+} = \left(\bar{a}^{+}_{\mathfrak{Y}\bar{a}x,}\ \mathfrak{z}^{+}{}_{\mathfrak{Y}\imath x,}\right)$, $\bar{a}^{-} = \left(\bar{a}^{-}_{\mathfrak{Y}\imath n,}\ \mathfrak{z}^{-}{}_{\mathfrak{Y}\bar{a}x,}\right)$, $\zeta > 0$ where, as shown in the equation at the bottom of the next page.

Then

$$\bar{a}^{-} \leq IVIFWDGBM (\varrho_1, \varrho_2, \ldots, \varrho_{\mathfrak{Y}}) \leq \bar{a}^{+}. \tag{25}$$

IV. MAGDM METHOD BASED ON IVIFWDBM AND IVIFDGBM OPERATORS

The MAGDM difficulties with the IVIF information will be processed using the IVIFWDBM and IVIFDGBM operators in this section.

A. DESCRIPTION OF THE MAGDM PROBLEMS

Consider a scenario where multiple decision makers denoted as $D = \{D_1, D_2, \ldots, D_t\}$, are tasked with evaluating a set of alternatives denoted as $X = \{X_1, X_2, \ldots, X_{\mathfrak{Y}}\}$, based on a set of attributes denoted as $C = \{C_1, C_2, \ldots, C_n\}$. Each decision maker provides evaluations in the form of Interval-Valued Intuitionistic Fuzzy Numbers (IVIFNs), represented as $\bar{a}^{k}_{\imath j} = \left(\left[\bar{a}^{lk}_{\imath j}, \bar{a}^{uk}_{\imath j}\right]\left[\mathfrak{z}^{lk}{}_{\imath j}, \mathfrak{z}^{uk}{}_{\imath j}\right]\right)$, where $\bar{a}^{lk}_{\imath j}$ $\bar{a}nd$ $\bar{a}^{uk}_{\imath j}$ represent lower and upper evaluations,

$$IVIFWDGBM^{\mathfrak{s},\mathfrak{b}} (\varrho_1, \varrho_2, \ldots, \varrho_{\mathfrak{Y}})$$
$$= \left(\left(1 - 1/\left(1 + \left(\frac{\mathfrak{Y}(\mathfrak{Y}-1)}{\mathfrak{s}+\mathfrak{b}} \times 1/\left(\sum_{\substack{\imath,j=1\\ \imath\neq j}}^{\mathfrak{Y}} \frac{1}{\left(w_{\imath}\left(\frac{\bar{a}^{l}_{\imath}}{1-\bar{a}^{l}_{\imath}}\right)^{\zeta} + w_j\left(\frac{\bar{a}^{l}_{j}}{1-\bar{a}^{l}_{j}}\right)^{\zeta}\right)}\right)\right)^{1/\zeta},\ \left(\frac{\mathfrak{Y}(\mathfrak{Y}-1)}{\mathfrak{s}+\mathfrak{b}} \times 1/\left(\sum_{\substack{\imath,j=1\\ \imath\neq j}}^{\mathfrak{Y}} \frac{1}{\left(w_{\imath}\left(\frac{\bar{a}^{u}_{\imath}}{1-\bar{a}^{u}_{\imath}}\right)^{\zeta} + w_j\left(\frac{\bar{a}^{u}_{j}}{1-\bar{a}^{u}_{j}}\right)^{\zeta}\right)}\right)\right)^{1/\zeta}\right)\right), \right.$$
$$\left. \left(\frac{1}{\left(1 + \left(\frac{\mathfrak{Y}(\mathfrak{Y}-1)}{\mathfrak{s}+\mathfrak{b}} \times 1/\left(\sum_{\substack{\imath,j=1\\ \imath\neq j}}^{\mathfrak{Y}} 1/\left(w_{\imath}\left(\frac{1-\mathfrak{z}^{l}_{\imath}}{\mathfrak{z}^{l}_{1}}\right)^{\zeta} + w_j\left(\frac{1-\mathfrak{z}^{l}_{j}}{\mathfrak{z}^{l}_{j}}\right)^{\zeta}\right)\right)\right)^{1/\zeta},\ \left(\frac{\mathfrak{Y}(\mathfrak{Y}-1)}{\mathfrak{s}+\mathfrak{b}} \times 1/\left(\sum_{\substack{\imath,j=1\\ \imath\neq j}}^{\mathfrak{Y}} 1/\left(w_{\imath}\left(\frac{1-\mathfrak{z}^{u}_{\imath}}{\mathfrak{z}^{u}_{1}}\right)^{\zeta} + w_j\left(\frac{1-\mathfrak{z}^{u}_{j}}{\mathfrak{z}^{u}_{j}}\right)^{\zeta}\right)\right)\right)^{1/\zeta}\right)}\right) \right) \tag{22}$$

respectively, for alternative X_{i} for attribute C_j as given by decision-maker D_k. The decision matrix $A^k = \left(\bar{a}^k_{\mathrm{i}j}\right)$ Contains these evaluations. Furthermore, each decision-maker is assigned a weight $\sum_{k=1}^{t} \zeta_k = 1, w = \{w_1, w_2, \ldots, w_n\}$, representing their importance in the decision-making process. Similarly, each attribute is assigned a weight $w_j \in [0, 1], \sum_{j=1}^{n} w_j = 1.$, reflecting their relative significance. Given this information, the task is to rank the alternatives based on the collective evaluations provided by the decision-makers and the assigned weights to the attributes. To fuse expert opinions while preserving individual preference uncertainty, the Dombi aggregation operator is applied.

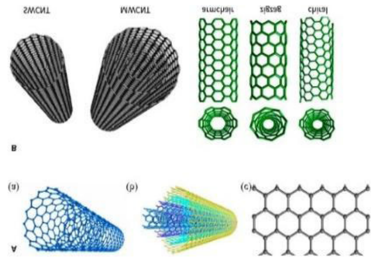

FIGURE 3. Smart sensors network.

The IVIFDBM aggregation of IVIFNs is mathematically formulated, as shown in the equation at the next page.

$$\bar{a}^{+}_{\mathfrak{Y}\bar{a}x} = 1/\left(1+\left(\frac{\mathfrak{Y}(\mathfrak{Y}-1)}{\mathscr{S}+\mathfrak{b}}\left(\frac{\underset{\mathrm{i}=1}{\mathrm{ma\eta}}\left(\varrho_{\mathrm{i}}\right)}{1-\underset{\mathrm{i}=1}{\mathrm{ma\eta}}\left(\varrho_{\mathrm{i}}\right)}\right)^{\zeta} \Big/ \left(\sum_{\substack{\mathrm{i},j=1\\ \mathrm{i}\neq j}}^{\mathfrak{Y}} 1/\left(\frac{\mathscr{S}}{w_{\mathrm{i}}}+\frac{\mathfrak{b}}{w_j}\right)\right)\right)^{1/\zeta}\right)$$

$$\mathfrak{z}^{+}{}_{\mathfrak{Y}\mathrm{i}_n} = 1-1\Big/\left(1+\left(\frac{\mathfrak{Y}(\mathfrak{Y}-1)}{\mathscr{S}+\mathfrak{b}}\times\left(\frac{1-\underset{\mathrm{i}=1}{\min}\left(\mathfrak{z}_{\mathrm{i}}\right)}{\underset{\mathrm{i}=1}{\min}\left(\mathfrak{z}_{\mathrm{i}}\right)}\right)^{\zeta}\times 1/\left(\sum_{\substack{\mathrm{i},j=1\\ \mathrm{i}\neq j}}^{\mathfrak{Y}} 1/\left(\frac{\mathscr{S}}{w_{\mathrm{i}}}+\frac{\mathfrak{b}}{w_j}\right)\right)\right)^{1/\zeta}\right) \quad \bar{a}^{-}_{\mathfrak{Y}\mathrm{i}_n} = 1/\left(1+\left(\frac{\mathfrak{Y}(\mathfrak{Y}-1)}{\mathscr{S}+\mathfrak{b}}\left(\frac{\underset{\mathrm{i}=1}{\min}\left(\varrho_{\mathrm{i}}\right)}{1-\underset{\mathrm{i}=1}{\min}\left(\varrho_{\mathrm{i}}\right)}\right)^{\zeta} \Big/ \left(\sum_{\substack{\mathrm{i},j=1\\ \mathrm{i}\neq j}}^{\mathfrak{Y}} 1/\left(\frac{\mathscr{S}}{w_{\mathrm{i}}}+\frac{\mathfrak{b}}{w_j}\right)\right)\right)^{1/\zeta}\right)$$

$$\mathfrak{z}^{-}{}_{\mathfrak{Y}\bar{a}x} = 1-1\Big/\left(1+\left(\frac{\mathfrak{Y}(\mathfrak{Y}-1)}{\mathscr{S}+\mathfrak{b}}\times\left(\frac{1-\underset{\mathrm{i}=1}{\mathrm{ma\eta}}\left(\mathfrak{z}_{\mathrm{i}}\right)}{\underset{\mathrm{i}=1}{\mathrm{ma\eta}}\left(\mathfrak{z}_{\mathrm{i}}\right)}\right)^{\zeta}\times 1/\left(\sum_{\substack{\mathrm{i},j=1\\ \mathrm{i}\neq j}}^{\mathfrak{Y}} \frac{1}{/}\left(\frac{\mathscr{S}}{w_{\mathrm{i}}}+\frac{\mathfrak{b}}{w_j}\right)\right)\right)^{1/\zeta}\right)$$

$$
\begin{aligned}
&IVIFDBM^{\mathfrak{s},\mathfrak{b}}\left(\varrho_1,\varrho_2,\ldots,\varrho_{\mathfrak{Y}}\right)\\
&=\left(\frac{1}{\left(1+\left(\frac{\mathfrak{Y}(\mathfrak{Y}-1)}{\mathfrak{s}+\mathfrak{b}}\times\frac{1}{\sum_{\substack{\mathrm{i},j=1\\ \mathrm{i}\neq j}}^{\mathfrak{Y}}\frac{1}{\mathfrak{s}\left(\frac{1-\bar{a}^{l}_{\mathrm{i}}}{\bar{a}^{l}_{\mathrm{i}}}\right)^{\zeta}+\mathfrak{b}\left(\frac{1-\bar{a}^{l}_{j}}{\bar{a}^{l}_{j}}\right)^{\zeta}}}\right)^{1/\zeta},\left(\frac{\mathfrak{Y}(\mathfrak{Y}-1)}{\mathfrak{s}+\mathfrak{b}}\times\frac{1}{\sum_{\substack{\mathrm{i},j=1\\ \mathrm{i}\neq j}}^{\mathfrak{Y}}\frac{1}{\mathfrak{s}\left(\frac{1-\bar{a}^{u}_{\mathrm{i}}}{\bar{a}^{u}_{\mathrm{i}}}\right)^{\zeta}+\mathfrak{b}\left(\frac{1-\bar{a}^{u}_{j}}{\bar{a}^{u}_{j}}\right)^{\zeta}}}\right)^{1/\zeta}\right)},\right.\\
&\left.1-\left(\frac{1}{\left(1+\left(\frac{\mathfrak{Y}(\mathfrak{Y}-1)}{\mathfrak{s}+\mathfrak{b}}\times\frac{1}{\sum_{\substack{\mathrm{i},j=1\\ \mathrm{i}\neq j}}^{\mathfrak{Y}}\frac{1}{\mathfrak{s}\left(\frac{\mathfrak{z}^{l}_{\mathrm{i}}}{1-\mathfrak{z}^{l}_{1}}\right)^{\zeta}+\mathfrak{b}\left(\frac{\mathfrak{z}^{l}_{j}}{1-\mathfrak{z}^{l}_{j}}\right)^{\zeta}}}\right)^{1/\zeta}\right)},\left(\frac{\mathfrak{Y}(\mathfrak{Y}-1)}{\mathfrak{s}+\mathfrak{b}}\times\frac{1}{\sum_{\substack{\mathrm{i},j=1\\ \mathrm{i}\neq j}}^{\mathfrak{Y}}\frac{1}{\mathfrak{s}\left(\frac{\mathfrak{z}^{u}_{\mathrm{i}}}{1-\mathfrak{z}^{u}_{1}}\right)^{\zeta}+\mathfrak{b}\left(\frac{\mathfrak{z}^{u}_{j}}{1-\mathfrak{z}^{u}_{j}}\right)^{\zeta}}}\right)^{1/\zeta}\right)\right)
\end{aligned}
$$

A similar formula is used for Geometric. After obtaining aggregated IVIFNs for all alternatives and criteria, the score function

$$S(\varrho) = \frac{(u_\varrho^l)(1-v_\varrho^l) + (u_\varrho^u)(1-v_\varrho^u)}{2}$$

where $S(\varrho) \in [-1,\ 1]$. and accuracy functions are used to rank the alternatives.

For example, consider two alternatives evaluated under a criterion: $A_1 = ([0.6,\ 0.7], [0.2,\ 0.3])$ and $A_2 = ([0.5,\ 0.6], [0.3,\ 0.4])$, Their score values would be:

$$S(A_1) = \frac{(0.6)(1-0.2) + (0.7)(1-0.3)}{2} = (0.6)(0.8) + \frac{(0.7)(0.7)}{2} = 0.485$$

$$S(A_2) = \frac{(0.5)(1-0.3) + (0.6)(1-0.4)}{2} = \frac{(0.5)(0.7) + (0.6)(0.6)}{2} = 0.355$$

Therefore, $A_1 \succ A_2$ representing a better option according to this criterion. This is repeated for all the criteria and combined to create a robust ranking. The incorporation of deep learning adds robustness to fuzzy input pattern feature extraction, allowing adaptive decision fusion in dynamic sensor network operations.

B. THE DECISION-MAKING METHOD BASED ON IVIFWDGM AND IVIFWDGBM OPERATORS

Step 1: Normalize the data used to make decisions. Benefit attributes and cost attributes are the two main categories of attribute values. It is necessary to normalize the decision-making matrices $A^k = [\bar{a}^k_{\imath j}]_{\mathfrak{Y}\times n}(k = 1, 2, \ldots, t)$ to remove the impact of different attribute types. We can transfer the attribute values of the cost type to the benefit type, and the modified decision matrices are expressed as $R^k = [r^k{}_{\imath j}]_{\mathfrak{Y}\times n}(k = 1, 2, \ldots, t), (\imath = 1, 2, \ldots, \mathfrak{Y}),\ j = 1, 2, \ldots, n)$, where

$$r^k{}_{\imath j} = \left(\left[\bar{a}^{lk}_{\imath j}, \bar{a}^{uk}_{\imath j}\right]\left[\mathfrak{z}^{lk}{}_{\imath j},\ \mathfrak{z}^{uk}{}_{\imath j}\right]\right) = \begin{cases} \left(\left[\bar{a}^{lk}_{\imath j}, \bar{a}^{uk}_{\imath j}\right]\left[\mathfrak{z}^{lk}{}_{\imath j},\ \mathfrak{z}^{uk}{}_{\imath j}\right]\right), \\ \text{if } C_j \text{ is } \mathfrak{z}enef\imath t\bar{a}ttr\imath\mathfrak{z}ute; \\ \left(\left[\mathfrak{z}^{lk}{}_{\imath j}, \mathfrak{z}^{uk}{}_{\imath j}\right]\left[\bar{a}^{lk}_{\imath j},\ \bar{a}^{uk}_{\imath j}\right]\right), \\ \imath f\, C_j \imath scost\ \bar{a}ttr\imath\mathfrak{z}ute \end{cases}$$

Step 2: Utilize the IVIFWDBM operator

$$r^k{}_{\imath} = \left(\left[\bar{a}^{lk}_{\imath j}, \bar{a}^{uk}_{\imath j}\right]\left[\mathfrak{z}^{lk}{}_{\imath j},\ \mathfrak{z}^{uk}{}_{\imath j}\right]\right) = IVIFDBM\left([r^k{}_{\imath 1}, r^k{}_{\imath 2}, \ldots, r^k{}_{\imath n}]\right)$$

or IVIFWDGBM operator

$$r^k{}_{\imath} = \left(\left[\bar{a}^{lk}_{\imath j}, \bar{a}^{uk}_{\imath j}\right]\left[\mathfrak{z}^{lk}{}_{\imath j},\ \mathfrak{z}^{uk}{}_{\imath j}\right]\right) = IVIFWDBM\left([r^k{}_{\imath 1}, r^k{}_{\imath 2}, \ldots, r^k{}_{\imath n}]\right)$$

to aggregate all the attributes to the overall preference value $r^k{}_{\imath}$ for each alternative for each decision-maker

Step 3: Utilize the IVIFWDBM operator

$$r_{\imath} = \left(\left[\bar{a}^{lk}_{\imath j}, \bar{a}^{uk}_{\imath j}\right]\left[\mathfrak{z}^{lk}{}_{\imath j},\ \mathfrak{z}^{uk}{}_{\imath j}\right]\right) = IVIFWDBM = \left([r^1{}_{\imath}, r^2{}_{\imath}, \ldots, r^t{}_{\imath}]\right)$$

Or IVIFWDGBM operator

$$r_{\imath} = \left(\left[\bar{a}^{lk}_{\imath j}, \bar{a}^{uk}_{\imath j}\right]\left[\mathfrak{z}^{lk}{}_{\imath j},\ \mathfrak{z}^{uk}{}_{\imath j}\right]\right) = IVIFWDGBM = \left([r^1{}_{\imath}, r^2{}_{\imath}, \ldots, r^t{}_{\imath}]\right)$$

$r_{\imath}\ (\imath = 1, 2, \ldots, \mathfrak{Y})$ is the aggregate overall preference value that must be determined?

Step 4: For each of the values $r_{\imath}\ (\imath = 1, 2, \ldots, \mathfrak{Y})$, compute the accuracy function $H\left(r_{\imath}\right)$ and the score function $S\left(r_{\imath}\right)$.

Step 5: Provide a scoring function $S\left(r_{\imath}\right)$ and an accuracy function $H\left(r_{\imath}\right)$ for each alternative $X = \left\{X_1, X_2, \ldots, X_{\mathfrak{Y}}\right\}$. Then, choose the best option or options.

Step 6: End.

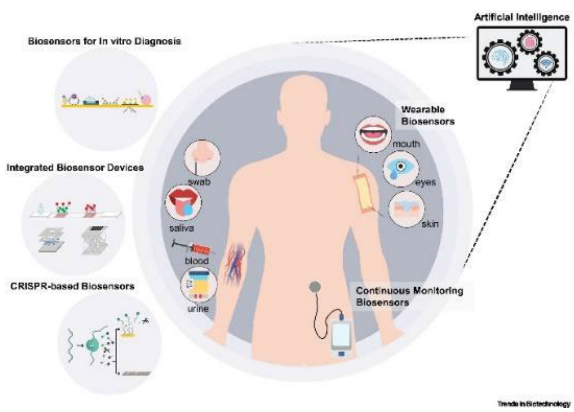

FIGURE 4. Carbon-based biosensors.

C. THEORETICAL DEPTH AND JUSTIFICATION OF D-IVIF AND D-IVIFDBM

The use of D-IVIFs in this research is motivated by their capacity to represent more detailed uncertainty than standard fuzzy models. In contrast to classical IFSs, D-IVIFs enable the MD and NMD to be represented as intervals, offering a more versatile structure to manage ambiguity and hesitation. Moreover, the operations of Dombi involve a significant tunable parameter that improves the sensitivity of aggregation so that decision-makers can adjust the softness or strictness of conjunction/disjunction operations.

In addition to further enhancing decision accuracy, this work suggests the D-IVIF DBM operator. The BM considers interdependence among attributes, which renders it very apt for complicated systems such as smart sensor networks in which criteria are normally interdependent. Coupled with Dombi operations, the operator stabilizes the effects of both predominant and secondary criteria during group decisions, which is particularly important under high dimensional data scenarios.

D. AI-DRIVEN ENVIRONMENTAL MONITORING AND HEALTHCARE DIAGNOSTICS SYSTEM OBJECTIVE

To create a decision-making system that uses smart sensor networks and carbon-based biosensors, powered by AI, to monitor environmental conditions and provide actionable insights for healthcare diagnostics:

1) SMART SENSOR NETWORKS

Smart Sensor Networks (SSNs) are advanced systems deployed in urban or industrial areas to monitor environmental parameters such as air quality, temperature, humidity, and pollutants using a combination of optical, chemical, and carbon-based biosensors. These networks detect harmful gases, particulate matter, and biological agents in real time, enabling data-driven decision-making for pollution control, public health, and industrial safety. Optical sensors measure light interactions for pollutant detection, chemical sensors identify specific gases like CO and NO_2, and carbon-based biosensors leverage nanomaterials like graphene to detect pathogens or biomarkers with high sensitivity. Integrated with AI and IoT, SSNs provide predictive analytics, real-time alerts, and actionable insights, ensuring safer environments, optimized industrial operations, and improved healthcare outcomes. Despite challenges like power consumption and data security, advancements in energy harvesting, encryption, and miniaturization are driving the future of scalable, efficient, and sustainable smart sensor networks. Deployed in urban or industrial areas to monitor air quality, temperature, humidity, and pollutants. Sensors include optical, chemical, and carbon-based.

2) CARBON-BASED BIOSENSORS

Carbon-based biosensors are advanced devices that utilize carbon nanomaterials, such as graphene or carbon nanotubes, to monitor biomarkers like glucose levels, heart rate, and oxygen saturation in real time, making them ideal for wearable or implantable healthcare applications. These biosensors offer high sensitivity and specificity, enabling the detection of pathogens, toxins, or environmental pollutants with exceptional accuracy. Their biocompatibility, flexibility, and miniaturization make them suitable for continuous health monitoring, early disease diagnosis, and environmental safety applications. By integrating with AI and IoT, carbon-based biosensors provide actionable insights, enhancing personalized healthcare and enabling rapid responses to environmental hazards. Their versatility and precision are driving innovations in medical diagnostics, wearable technology, and environmental monitoring. Wearable or implantable biosensors for monitoring biomarkers (e.g., glucose levels, heart rate, oxygen saturation). High-sensitivity detection of pathogens or toxins in the environment.

3) AI AND DEEP LEARNING MODELS

AI and deep learning models play a pivotal role in smart sensor networks by enabling real-time data analysis and pattern recognition to extract meaningful insights from vast amounts of sensor data. These models, such as Convolutional Neural Networks (CNNs) for image-based data and Recurrent Neural Networks (RNNs) for time-series data, identify trends, anomalies, and correlations in environmental and health-related metrics. By leveraging predictive analytics, AI can forecast environmental risks (e.g., air pollution spikes) and health risks (e.g., disease outbreaks or abnormal biomarkers), allowing for proactive decision-making and timely interventions. This integration of AI enhances the efficiency, accuracy, and scalability of smart sensor networks, transforming raw data into actionable intelligence for safer and healthier environments. Real-time data analysis and pattern recognition. Predictive analytics for environmental and health risks.

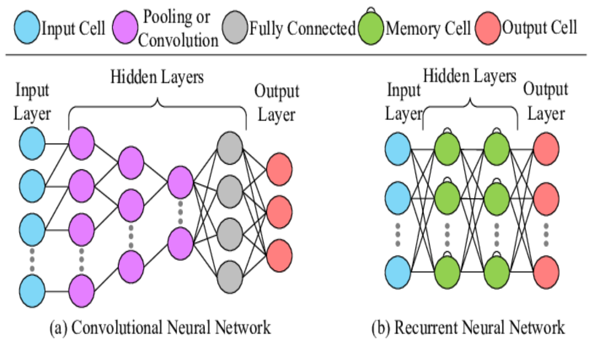

FIGURE 5. AI and deep learning models.

4) DECISION-MAKING ENGINE

The Decision-Making Engine is a critical component of smart sensor networks that integrates sensor data with AI insights to generate actionable recommendations. By analyzing real-time data from environmental and biological sensors, the engine identifies patterns, detects anomalies, and predicts risks using advanced AI models like CNNs and RNNs. It then translates these insights into practical actions, such as issuing alerts for pollution spikes, optimizing industrial processes, or providing personalized health recommendations. This engine ensures timely, data-driven decisions, enhancing safety, efficiency, and overall system performance.

E. STEP-BY-STEP DECISION-MAKING PROCESS

1) DATA COLLECTION

Environmental Data: Smart sensors collect real-time data on air quality, temperature, humidity, and pollutant levels.

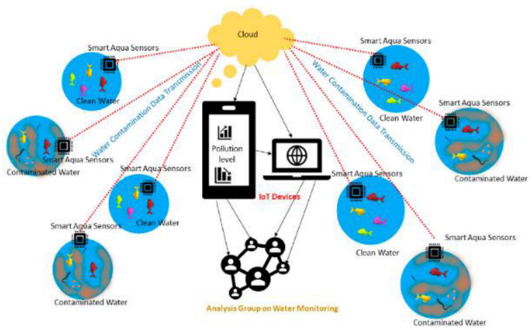

FIGURE 6. AI and deep learning models.

Biological Data: Carbon-based biosensors collect health-related data (e.g., glucose levels, and heart rate) from individuals in the area.

2) DATA PREPROCESSING

Clean and normalize data to remove noise and outliers. Extract relevant features (e.g., a spike in pollutant levels, abnormal heart rate patterns).

3) AI ANALYSIS

Use CNNs to analyze optical data from sensors (e.g., detecting particulate matter in the air). Use RNNs to analyze time-series data (e.g., trends in air quality or heart rate variability). Use Reinforcement Learning to optimize sensor placement and data collection strategies.

4) DECISION-MAKING ENGINE

Environmental Monitoring:

If pollutant levels exceed safe thresholds, the system triggers alerts for local authorities and recommends actions (e.g., evacuate the area, and reduce industrial activity). Predict future environmental risks (e.g., smog formation) using predictive analytics.

Healthcare Diagnostics:

If biosensors detect abnormal health metrics (e.g., high glucose levels, irregular heart rate), the system alerts the individual and healthcare providers. Recommend personalized interventions (e.g., take medication, visit a doctor).

5) INTEGRATION WITH IoT AND CLOUD COMPUTING

Transmit data to cloud platforms for storage and further analysis. Use edge computing for real-time decision-making in critical situations.

6) SENSITIVITY ANALYSIS

To determine how resilient, the supplier rankings are to modifications in the weights given to the criterion or in the assessment values, perform a sensitivity analysis. This helps in understanding the decision-making process's stability and dependability.

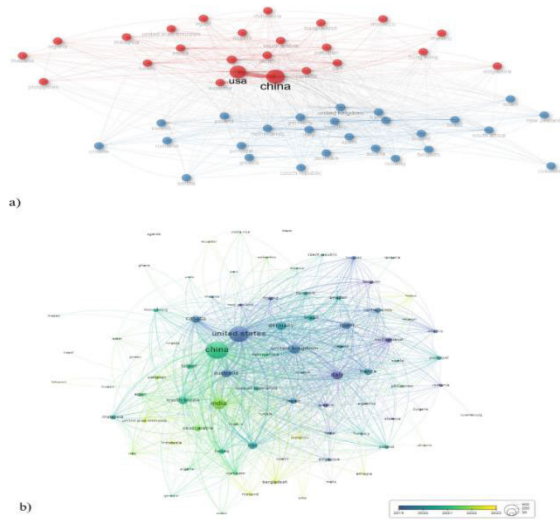

FIGURE 7. AI-driven environmental monitoring and healthcare diagnostics system.

V. DECISION-MAKING

Based on the rankings, the findings of the sensitivity analysis, and the degree of alignment with the business's operational and strategic goals, choose an AI model.

A. NUMERICAL APPLICATION OF AI-DRIVEN ENVIRONMENTAL MONITORING AND HEALTHCARE DIAGNOSTICS SYSTEM

In an industrial area, a smart sensor network detects a sudden spike in carbon monoxide (CO) levels, while carbon-based biosensors worn by workers simultaneously record elevated heart rates and low oxygen saturation. AI models analyze this data, identifying a direct correlation between environmental hazards and health risks. The system immediately alerts factory managers to shut down machinery and ventilate the area, while notifying workers to evacuate and seek medical attention. Additionally, predictive analytics forecast potential long-term health impacts, recommending follow-up medical checks. This integrated approach prevents emergencies, ensures worker safety, and showcases the power of combining smart sensor networks and AI for real-time, data-driven decision-making.

Example 1: We consider four AI-driven models (alternatives) for environmental monitoring and healthcare diagnostics: **A1:** CNN-Based Model, **A2:** LSTM-Based Model, **A3:** Hybrid CNN-LSTM Model, **A4:** Transformer- Based Model. The models are evaluated based on four performance criteria: **C1:** Accuracy (%), **C2:** Sensitivity (%), **C3:** Computational Efficiency (ms), **C4:** Energy Consumption (J).

VI. EXPERIMENTAL SETUP

To assess the effectiveness and robustness of the suggested IVIFDBM–based MAGDM model coupled with deep learning, an extensive experimental study was undertaken. The

TABLE 2. A general IVIF DM A^1 given by D_1.

	Accuracy ₵$_1$				Sensitivity ₵$_2$				Computational Efficiency (₵$_3$)				Energy Consumption (₵$_4$)			
	MD		NMD		MD		NMD		MD		NMD		MD		NMD	
	L	U	L	U	L	U	L	U	L	U	L	U	L	U	L	U
Ӿ$_1$(CNN)	0.45	0.63	0.25	0.35	0.24	0.43	0.37	0.42	0.25	0.39	0.37	0.45	0.36	0.48	0.46	0.57
Ӿ$_2$(LSTM)	0.25	0.43	0.33	0.54	0.21	0.48	0.37	0.45	0.34	0.51	0.34	0.44	0.23	0.34	0.45	0.56
Ӿ$_3$ (Transformer)	0.34	0.47	0.21	0.43	0.42	0.54	0.27	0.35	0.24	0.45	0.45	0.65	0.25	0.35	0.43	0.54
Ӿ$_4$ (CNN-LSTM)	0.15	0.51	0.23	0.32	0.24	0.42	0.45	0.57	0.43	0.67	0.34	0.43	0.25	0.52	0.24	0.34

TABLE 3. A general IVIF DM A^2A^2 given by D_2.

	Accuracy ₵$_1$				Sensitivity ₵$_2$				Computational Efficiency (₵$_3$)				Energy Consumption (₵$_4$)			
	MD		NMD		MD		NMD		MD		NMD		MD		NMD	
	L	U	L	U	L	U	L	U	L	U	L	U	L	U	L	U
Ӿ$_1$(CNN)	.25	0.35	0.32	0.45	0.32	0.54	0.46	0.57	0.24	0.34	0.27	0.36	0.33	0.45	0.35	0.52
Ӿ$_2$(LSTM)	0.35	0.43	0.43	0.57	0.45	0.54	0.37	0.64	0.35	0.53	0.23	0.32	0.38	0.45	0.42	0.56
Ӿ$_3$ (Transformer)	0.23	0.36	0.35	0.42	0.28	0.47	0.39	0.53	0.26	0.46	0.45	0.53	0.34	0.45	0.32	0.56
Ӿ$_4$ (CNN-LSTM)	0.37	0.43	0.23	0.32	0.43	0.55	0.34	0.43	0.27	0.56	0.34	0.48	0.26	0.46	0.45	0.53

TABLE 4. A general IVIF DM A^3A^3 given by D_3.

	Accuracy ₵$_1$				Sensitivity ₵$_2$				Computational Efficiency (₵$_3$)				Energy Consumption (₵$_4$)			
	MD		NMD		MD		NM D		MD		NMD		MD		NMD	
	L	U	L	U	L	U	L	U	L	U	L	U	L	U	L	U
Ӿ$_1$(CNN)	0.35	0.45	0.26	0.43	0.35	0.45	0.34	0.54	0.43	0.54	0.38	0.48	0.34	0.45	0.26	0.47
Ӿ$_2$(LSTM)	0.24	0.36	0.38	0.46	0.34	0.43	0.35	0.45	0.34	0.45	0.45	0.54	0.34	0.48	0.45	0.57
Ӿ$_3$ (Transformer)	0.38	0.45	0.37	0.46	0.23	0.42	0.34	0.45	0.27	0.47	0.34	0.43	0.32	0.45	0.39	0.48
Ӿ$_4$ (CNN-LSTM)	0.25	0.35	0.43	0.54	0.35	0.45	0.34	0.54	0.36	0.64	0.34	0.54	0.28	0.52	0.34	0.52

experiments targeted a real-life decision-making case about carbon-based biosensor deployment in a smart healthcare setting.

A. DATASET AND CASE CONTEXT

The case study entailed four alternatives (A_1 to A4) with varying biosensor prototypes, and seven evaluation criteria (C_1 to C4), including Accuracy, Sensitivity, Computational efficiency, and Energy consumption. The decision matrix was constructed through four expert decision-maker evaluations, each with interval-valued intuitionistic fuzzy assessments. For performance benchmarking, the proposed model was compared with traditional MAGDM approaches such as Interval-valued intuitionistic fuzzy Dombi weighted averaging (IVIFDWA) [29], Interval-valued intuitionistic fuzzy Dombi weighted geometric (IVIFDWG) [29] Interval-valued intuitionistic fuzzy weighted Heronian mean (IVIFWHM) [29], Interval-valued intuitionistic fuzzy weighted Aczel-Alsina averaging (IVIFWAA) [30], Interval-valued intuitionistic fuzzy weighted Aczel-Alsina geometric (IVIFAAWG) [30], and Interval-valued intuitionistic fuzzy BM (IVIFB) [] operator. Evaluation metrics included the weighted Similarity (WS) index, computational time, and sensitivity to expert disagreement.

TABLE 5. IVIF aggregated decision matrix.

	Accuracy ₵$_1$				Sensitivity ₵$_2$				Computational Efficiency ₵$_3$			
	MD		NMD		MD		NMD		MD		NMD	
	L	U	L	U	L	U	L	U	L	U	L	U
Ӿ$_1$(CNN)	0.171	0.1778	0.9049	0.8281	0.1843	0.2106	0.8488	0.7818	0.15086	0.15779	0.8714	0.8071
Ӿ$_2$(LSTM)	0.1963	0.2368	0.8634	0.7664	0.2165	0.2205	0.8594	0.7842	0.2274	0.2151	0.8816	0.8217
Ӿ$_3$ (Transformer)	0.1590	0.2038	0.9065	0.8062	0.1774	0.2132	0.8882	0.8254	0.1599	0.2130	0.8510	0.7721
Ӿ$_4$ (CNN-LSTM)	0.1854	0.2273	0.9057	0.8330	0.2151	0.2156	0.8523	0.7628	0.1866	0.1114	0.8676	0.7787
Energy Consumption ₵$_4$												
	MD		NMD									
	L	U	L	U								
Ӿ$_1$(CNN)	0.2035	0.2066	0.8793	0.7794								
Ӿ$_2$(LSTM)	0.2096	0.2053	0.8092	0.7347								
Ӿ$_3$ (Transformer)	0.1929	0.216	0.8470	0.7693								
Ӿ$_4$ (CNN-LSTM)	0.1665	0.1765	0.8879	0.8085								

TABLE 6. Ranking of AI models based on performance scores.

Alternative	Score Value by using IVIFWDBM	Score Value by using IVIFWGDBM
Ӿ$_1$(CNN)	0.140381	0.075903
Ӿ$_2$(LSTM)	0.150973	0.094023
Ӿ$_3$ (Transformer)	0.135398	0.112807
Ӿ$_4$ (CNN-LSTM)	0.182854	0.029784

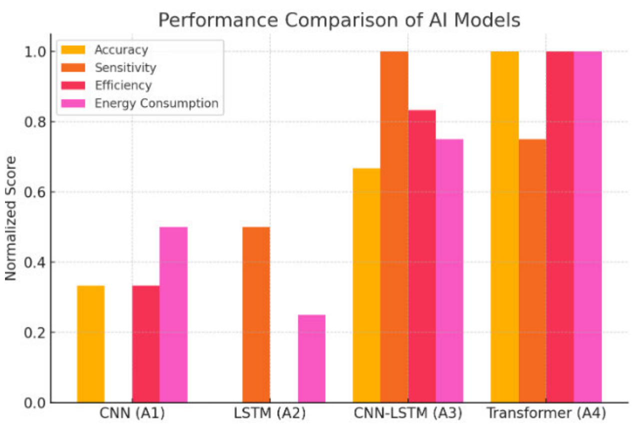

FIGURE 8. Graphical visualization of performance comparison of AI models.

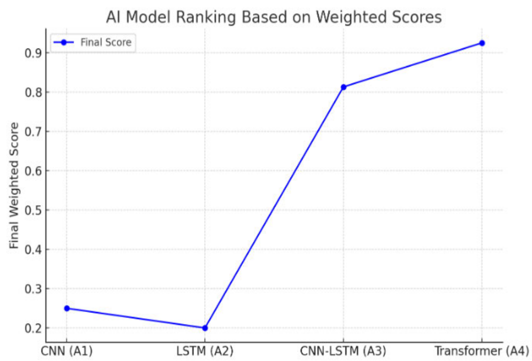

FIGURE 9. Graphical visualization of AI models ranking.

VII. RESULT DISCUSSION AND COMPARISON OF IVIFDBM OPERATOR WITH VARIOUS EXISTING AGGREGATION

The presented IVIFDBM model compares well with conventional IVIF and PFS-based aggregation methods regarding uncertainty processing and consistent ranking of decisions. The use of the Dombi parameter grants extra flexibility for adjusting the nature of aggregation behavior, which isn't achievable in the case of conventional t-norm and t-conorm functions. This contributes to the unique suitability of the model for tasks in optoelectronic devices, where decision-making needs to be robust, yet sensitive towards real-time updates in data.

The IVIFDBM operator is extensively compared and compared with several current aggregation techniques for AI-driven environmental monitoring and medical diagnostics systems in this section. The comparison is based on the score values that were obtained using various operators, such as the following: Interval-valued intuitionistic fuzzy Dombi weighted averaging (IVIFDWA) [48], Interval-valued intuitionistic fuzzy Dombi weighted geometric (IVIFDWG) [48]Interval-valued intuitionistic fuzzy weighted Heronian mean (IVIFWHM) [29], Interval-valued intuitionistic fuzzy weighted Aczel-Alsina averaging (IVIFWAA) [49], Interval-valued intuitionistic fuzzy weighted Aczel-Alsina geometric

TABLE 7. Comparative analysis of the proposed IVIFDBM operator with existing operators for AI-driven environmental monitoring and healthcare diagnostics system.

Alternative	Score Value by using IVIFDWA operator	Score Value by using IVIFDWG operator	Score Value by using the IVIFWHM operator	Score Value by using IVIFWAA operator	Score Value by using the IVIFWAG operator	Score Value by using IVIFB
χ_1	0.1591	0.2724	0.75314	0.2351	0.2213	0.2435
χ_2	0.1653	0.2651	0.70678	0.1881	0.1814	0.3447
χ_3	0.2212	0.2568	0.7345	0.1929	0.1810	0.3449
χ_4	0.14503	0.3273	0.7427	0.2785	0.2600	0.3454

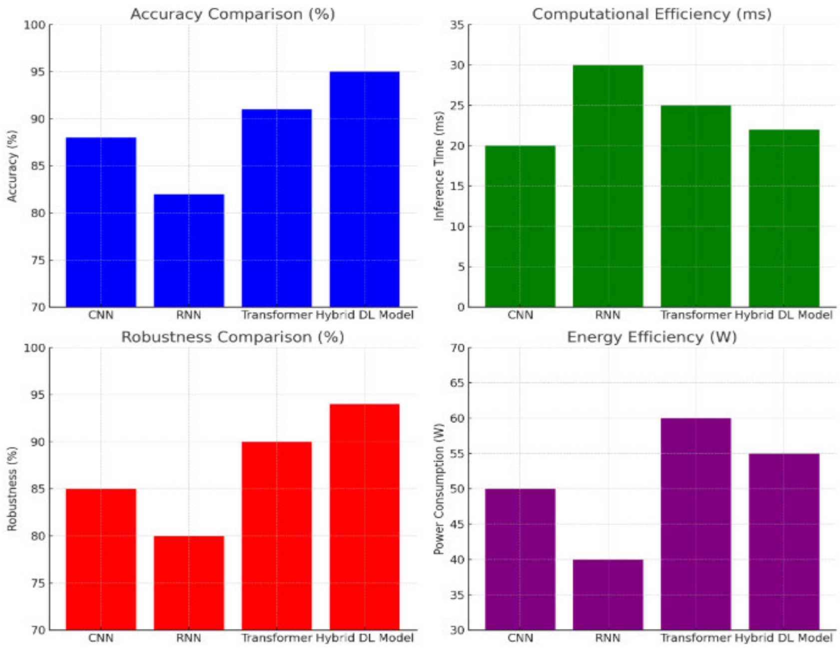

FIGURE 10. Graphical representation comparing the four AI models based on accuracy, computational efficiency, robustness, and energy consumption.

TABLE 8. Comparison of proposed approach with existing approaches.

Approach	Advantages	Dis-advantages
Proposed AI-Driven System (Deep Learning-based Decision Making)	High adaptability, dynamic learning capability, real-time decision-making	Requires high computational resources
Traditional Fuzzy Logic MCDM	Handles uncertainty well, interpretable	Limited adaptability to real-time data
Rule-Based Expert Systems	Clear rules, domain-specific expertise	Lacks self-learning ability
Machine Learning-Based Approaches	Good for classification, predictive modeling	Feature selection is crucial, not always real-time

(IVIFAAWG) [49], and Interval-valued intuitionistic fuzzy BM (IVIFB) [] operator.

When it comes to combining assessments from AI-driven environmental monitoring and healthcare diagnostics system criteria, the IVIFDBM operator performs exceptionally well. By integrating AI-driven methodologies, the proposed framework effectively addresses the complexities and uncertainties associated with real-time environmental monitoring and healthcare diagnostics. The deep learning approach enables precise data processing, pattern recognition, and predictive analytics, optimizing the performance and efficiency of smart sensor networks and more accurate decision support when compared to other operators.

IVIFDWA Operator: In situations where the weights assigned to criteria are dynamic and subject to change, the IVIFDWA operator performs competitively when aggregating evaluations. In contrast to IVIFDBM, it might, however, show shortcomings in managing ambiguity and uncertainty in evaluation data.

IVIFDWG Operator: The geometric mean aggregation method, which is the focus of the IVIFDWG operator, might be useful in situations where striking a balance between robustness and precision is essential. IVIFDWG might not be able to fully capture the range of uncertainties included in supplier selection procedures, even though it might yield good findings in some situations.

IVIFWHM Operator: To properly capture the interrelationships across criteria, the IVIFWHM operator makes use of the Heronian mean aggregation method. Although the Heronian mean has theoretical benefits, its practical applicability in AI-driven environmental monitoring and healthcare diagnostics systems may be limited when compared to IVIFDBM.

IVIFWAA Operator: The weighted arithmetic aggregation method, which enables decision-makers to give various criteria differing degrees of importance, is highlighted by the IVIFWAA operator. IVIFWAA allows for flexibility

$$
\begin{aligned}
&IVIFDBM^{\mathfrak{s},0}\left(\varrho_1,\varrho_2,\ldots,\varrho_{\mathfrak{Y}}\right)\\
&=\lim_{\mathfrak{b}\to 0}\left(\begin{matrix}
1/\begin{pmatrix}
1+\left(1/\left(\dfrac{\mathfrak{Y}(\mathfrak{Y}-1)}{\mathfrak{s}+\mathfrak{b}}\times\left(\sum_{\substack{\mathfrak{i},j=1\\ \mathfrak{i}\neq j}}^{\mathfrak{Y}}\dfrac{1}{\left(\mathfrak{s}\left(\dfrac{1-\bar{a}^{l}_{\mathfrak{i}}}{\bar{a}^{l}_{\mathfrak{i}}}\right)^{\zeta}+\mathfrak{b}\left(\dfrac{1-\bar{a}^{l}_{j}}{\bar{a}^{l}_{j}}\right)^{\zeta}\right)}\right)\right)^{1/\zeta}\right)\\
\left(1/\left(\dfrac{\mathfrak{Y}(\mathfrak{Y}-1)}{\mathfrak{s}+\mathfrak{b}}\times\left(\sum_{\substack{\mathfrak{i},j=1\\ \mathfrak{i}\neq j}}^{\mathfrak{Y}}1/\left(\mathfrak{s}\left(\dfrac{\mathfrak{z}^{u}_{\mathfrak{i}}}{1-\mathfrak{z}^{u}_{1}}\right)^{\zeta}+\mathfrak{b}\left(\dfrac{\mathfrak{z}^{u}_{j}}{1-\mathfrak{z}^{u}_{j}}\right)^{\zeta}\right)\right)\right)^{1/\zeta}\right)
\end{pmatrix}
\end{matrix}\right.,\\
&\qquad 1-\left(\begin{matrix}
\dfrac{1}{\left(1+\left(\left(\dfrac{\mathfrak{Y}(\mathfrak{Y}-1)}{\mathfrak{s}+\mathfrak{b}}\times\dfrac{1}{\left(\mathfrak{s}\left(\dfrac{1-\bar{a}^{u}_{\mathfrak{i}}}{\bar{a}^{u}_{\mathfrak{i}}}\right)^{\zeta}+\mathfrak{b}\left(\dfrac{1-\bar{a}^{u}_{j}}{\bar{a}^{u}_{j}}\right)^{\zeta}\right)}\right)\left(\sum_{\substack{\mathfrak{i},j=1\\ \mathfrak{i}\neq j}}^{\mathfrak{Y}}\dfrac{1}{\left(\mathfrak{s}\left(\dfrac{\mathfrak{z}^{l}_{\mathfrak{i}}}{1-\mathfrak{z}^{l}_{1}}\right)^{\zeta}+\mathfrak{b}\left(\dfrac{\mathfrak{z}^{l}_{j}}{1-\mathfrak{z}^{l}_{j}}\right)^{\zeta}\right)}\right)\right)^{1/\zeta}\right)},\\
\left(1/\left(\dfrac{\mathfrak{Y}(\mathfrak{Y}-1)}{\mathfrak{s}+\mathfrak{b}}\times\left(\sum_{\substack{\mathfrak{i},j=1\\ \mathfrak{i}\neq j}}^{\mathfrak{Y}}\dfrac{1}{\left(\mathfrak{s}\left(\frac{\mathfrak{z}^{u}_{\mathfrak{i}}}{1-\mathfrak{z}^{u}_{1}}\right)^{\zeta}+\mathfrak{b}\left(\frac{\mathfrak{z}^{u}_{j}}{1-\mathfrak{z}^{u}_{j}}\right)^{\zeta}\right)}\right)\right)\right)^{1/\zeta}
\end{matrix}\right)
\end{aligned}
$$

$$
\begin{aligned}
&=\left(1/\begin{pmatrix}
1+\left(\left(\frac{\mathfrak{Y}(\mathfrak{Y}-1)}{\mathfrak{s}}\right)^{1/\zeta}\times 1/\left(\sum_{\substack{\mathfrak{i},j=1\\ \mathfrak{i}\neq j}}^{\mathfrak{Y}}\frac{1}{\left(\mathfrak{s}\left(\frac{1-\bar{a}^{l}_{\mathfrak{i}}}{\bar{a}^{l}_{\mathfrak{i}}}\right)^{\zeta}\right)}\right)\right)^{1/\zeta}\\
\left(\left(\frac{\mathfrak{Y}(\mathfrak{Y}-1)}{\mathfrak{s}}\right)^{1/\zeta}\times 1/\left(\sum_{\substack{\mathfrak{i},j=1\\ \mathfrak{i}\neq j}}^{\mathfrak{Y}}\frac{1}{\left(\mathfrak{s}\left(\frac{1-\bar{a}^{u}_{\mathfrak{i}}}{\bar{a}^{u}_{\mathfrak{i}}}\right)^{\zeta}\right)}\right)\right)^{1/\zeta}
\end{pmatrix}\right.,\\
&\qquad 1-\left.\begin{pmatrix}
\frac{1}{1}+\left(\left(\frac{\mathfrak{Y}(\mathfrak{Y}-1)}{\mathfrak{s}}\right)^{1/\zeta}\times 1/\left(\sum_{\mathfrak{i}=1}^{\mathfrak{Y}}\frac{1}{\left(\mathfrak{s}\left(\frac{\mathfrak{z}^{l}_{\mathfrak{i}}}{1-\mathfrak{z}^{l}_{1}}\right)^{\zeta}\right)}\right)\right)^{1/\zeta}\\
\left(\left(\frac{\mathfrak{Y}(\mathfrak{Y}-1)}{\mathfrak{s}}\right)^{1/\zeta}\times 1/\left(\sum_{\mathfrak{i}=1}^{\mathfrak{Y}}\frac{1}{\left(\mathfrak{s}\left(\frac{\mathfrak{z}^{u}_{\mathfrak{i}}}{1-\mathfrak{z}^{u}_{1}}\right)^{\zeta}\right)}\right)\right)^{1/\zeta}
\end{pmatrix}\right)
\end{aligned}
$$

in weighing criteria, although it might not be as good as IVIFDBM at handling the intricacies of ambiguous and unclear information.

IVIFWAG Operator: The weighted geometric aggregation approach is integrated into the IVIFWAG operator, which can be useful in situations where accuracy and resilience are crucial. In contrast to IVIFDBM, IVIFWAG might find it difficult to capture the inherent ambiguity and uncertainties in AI-driven environmental monitoring and healthcare diagnostics systems.

IVIFB Operator: Based on the BM aggregation method, the IVIFB operator seeks to account for the ambiguity and uncertainty in evaluation data while capturing the links between criteria. Although IVIFB has theoretical benefits, its usefulness and practicality in supplier selection may differ from those of IVIFDBM.

In conclusion, the IVIFDBM operator emerges as the preferred choice for AI-driven environmental monitoring and healthcare diagnostics systems offering superior performance in aggregating evaluations across multiple criteria. While other existing aggregation methods may provide competitive results in specific contexts, IVIFDBM consistently captures the complexities of uncertain and vague information inherent in AI-driven environmental monitoring and healthcare diagnostics systems.

A. ADVANTAGES OF THE PROPOSED MODEL

The IVIFDBM model has the following significant benefits over other decision-making models. First, the model efficiently handles ambiguity, hesitation, and contradictory expert opinions using IVIF information, which yields a richer

$$
\begin{aligned}
&IVIFDBM^{1,0}\left(\varrho_1,\varrho_2,\ldots,\varrho_{\mathfrak{Y}}\right)\\
&=\left(1\Big/\left(\begin{array}{c}1+\left(\left(\mathfrak{Y}\left(\mathfrak{Y}-1\right)\right)^{1/\zeta}\Big/\left(\sum_{\mathfrak{i}=1}^{\mathfrak{Y}}\frac{1}{\left(\left(\frac{1-\bar{a}_{\mathfrak{i}}^{l}}{\bar{a}_{\mathfrak{i}}^{l}}\right)^{\zeta}\right)}\right)\right)^{1/\zeta},\\ 1+\left(\left(\mathfrak{Y}\left(\mathfrak{Y}-1\right)\right)^{1/\zeta}\Big/\left(\sum_{\mathfrak{i}=1}^{\mathfrak{Y}}\frac{1}{\left(\left(\frac{1-\bar{a}_{\mathfrak{i}}^{u}}{\bar{a}_{\mathfrak{i}}^{u}}\right)^{\zeta}\right)}\right)\right)^{1/\zeta}\end{array}\right)\right),\; 1-\left(\frac{1}{\left(\begin{array}{c}\left(1+\left(\left(\mathfrak{Y}\left(\mathfrak{Y}-1\right)\right)^{1/\zeta}\Big/\left(\sum_{\mathfrak{i}=1}^{\mathfrak{Y}}\frac{1}{\left(\left(\frac{\text{ʒ}_{\mathfrak{i}}^{l}}{1-\text{ʒ}_{1}^{l}}\right)^{\zeta}\right)}\right)\right)\right)^{1/\zeta},\\ \left(\left(\mathfrak{Y}\left(\mathfrak{Y}-1\right)\right)^{1/\zeta}\Big/\left(\sum_{\mathfrak{i}=1}^{\mathfrak{Y}}\frac{1}{\left(\left(\frac{\text{ʒ}_{\mathfrak{i}}^{u}}{1-\text{ʒ}_{1}^{u}}\right)^{\zeta}\right)}\right)\right)^{1/\zeta}\end{array}\right)}\right)
\end{aligned}
$$

,

$$
\begin{aligned}
&IVIFDBM^{0,\text{ƃ}}\left(\varrho_1,\varrho_2,\ldots,\varrho_{\mathfrak{Y}}\right)\\
&=\left(1\Big/\left(\begin{array}{c}\left(\begin{array}{c}1+\left(\frac{\mathfrak{Y}\left(\mathfrak{Y}-1\right)}{\text{ƃ}}\right)^{1/\zeta}\\ \times 1\Big/\left(\sum_{\substack{\mathfrak{i},j=1\\ \mathfrak{i}\neq j}}^{\mathfrak{Y}}\frac{1}{\left(\text{ƃ}\left(\frac{1-\bar{a}_{j}^{l}}{\bar{a}_{j}^{l}}\right)^{\zeta}\right)}\right)\end{array}\right)^{1/\zeta},\\ \left(\begin{array}{c}1+\left(\frac{\mathfrak{Y}\left(\mathfrak{Y}-1\right)}{\text{ƃ}}\right)^{1/\zeta}\\ \times 1\Big/\left(\sum_{\substack{\mathfrak{i},j=1\\ \mathfrak{i}\neq j}}^{\mathfrak{Y}}\frac{1}{\left(\text{ƃ}\left(\frac{1-\bar{a}_{j}^{u}}{\bar{a}_{j}^{u}}\right)^{\zeta}\right)}\right)\end{array}\right)^{1/\zeta}\end{array}\right)\right),1-\left(\frac{1}{\left(\begin{array}{c}\left(\left(\begin{array}{c}1+\left(\frac{\mathfrak{Y}\left(\mathfrak{Y}-1\right)}{\text{ƃ}}\right)^{1/\zeta}\\ \times 1\Big/\left(\sum_{\substack{\mathfrak{i},j=1\\ \mathfrak{i}\neq j}}^{\mathfrak{Y}}\frac{1}{\left(\text{ƃ}\left(\frac{\text{ʒ}_{j}^{l}}{1-\text{ʒ}_{j}^{l}}\right)^{\zeta}\right)}\right)\end{array}\right)^{1/\zeta},\right)\\ \left(\begin{array}{c}1+\left(\frac{\mathfrak{Y}\left(\mathfrak{Y}-1\right)}{\text{ƃ}}\right)^{1/\zeta}\\ \times 1\Big/\left(\sum_{\substack{\mathfrak{i},j=1\\ \mathfrak{i}\neq j}}^{\mathfrak{Y}}\frac{1}{\left(\text{ƃ}\left(\frac{\text{ʒ}_{j}^{u}}{1-\text{ʒ}_{j}^{u}}\right)^{\zeta}\right)}\right)\end{array}\right)^{1/\zeta}\end{array}\right)}\right)
\end{aligned}
$$

and more flexible uncertainty representation. Second, the Dombi operation laws add an adjustable parameter to the model, which increases the model's flexibility to suit different decision-making behaviors and facilitates more personalized aggregation. Third, the BM operator preserves interdependencies between decision attributes, ensuring that mutual impact between criteria is properly taken into account something usually neglected in traditional models. Fourth, through the incorporation of this fuzzy system with deep learning elements, the model enables intelligent pattern detection and real-time adjustability, essential in applications such as optoelectronic device innovation. Finally, the model is scalable and resilient, which allows it to be applicable in small and big-sized multi-attribute group decision-making issues in dynamic and data-intensive settings.

VIII. IMPLICATIONS, APPLICATIONS, AND LIMITATIONS

A. REAL-WORLD APPLICATIONS

The suggested D-IVIFDBM-based MAGDM structure has great promise for practical implementation in fields depending significantly on smart sensing and expedient decision-making. In smart healthcare systems, the model is capable of early disease detection with biosensors through aggregating incomplete and uncertain physiological information from multiple diagnostic sources. In environmental monitoring, it is capable of instant evaluation of air or water quality based on fuzzy or conflicting results from sensor networks. Likewise, in industrial automation, the model facilitates optimized control decisions by operating on multi-sensory input under uncertain circumstances, improving safety as well as efficiency.

Deep learning fusion with fuzzy aggregation improves the system's ability to learn from past sensor information and support adaptive behavior in dynamic environments. Optoelectronic devices benefit from this adaptability, where real-time sensitivity and dynamic feature extraction are key.

B. IMPLICATIONS

The results show that integrating fuzzy modeling with advanced learning techniques has greatly enhanced decision precision, dependability, and flexibility. This adds to the literature on hybrid decision-making systems and provides initial groundwork for future research in AI-based fuzzy control systems, particularly in fields where there is inherent uncertainty.

C. LIMITATIONS AND CHALLENGES

While the suggested model has advantages, it has some limitations as well. Its major limitation is computational complexity from incorporating interval-valued data, fuzzy operators, and deep learning concepts, which might need tremendous processing power in real-time environments. Parameter adjustments in Dombi operators and deep learning processes may also compromise consistency if not kept under check. A further limitation is a reliance on expert-set criteria

$$IVIFDBM^{1,1}\left(\varrho_1, \varrho_2, \ldots, \varrho_{\mathfrak{Y}}\right)$$

$$= \left(1/\left(\left(\left(1+\left(\frac{\mathfrak{Y}\left(\mathfrak{Y}-1\right)}{2}\right)^{1/\zeta} \times 1/\left(\sum_{\substack{\mathrm{i},j=1\\ \mathrm{i}\neq j}}^{\mathfrak{Y}} \frac{1}{\left(\left(\frac{1-\bar{a}^l_{\mathrm{i}}}{\bar{a}^l_{\mathrm{i}}}\right)^{\zeta}+\left(\frac{1-\bar{a}^l_j}{\bar{a}^l_j}\right)^{\zeta}\right)} \right) \right)^{1/\zeta} \right), \left(1+\left(\frac{\mathfrak{Y}\left(\mathfrak{Y}-1\right)}{2}\right)^{1/\zeta} \times 1/\left(\sum_{\substack{\mathrm{i},j=1\\ \mathrm{i}\neq j}}^{\mathfrak{Y}} \frac{1}{\left(\left(\frac{1-\bar{a}^u_{\mathrm{i}}}{\bar{a}^u_{\mathrm{i}}}\right)^{\zeta}+\left(\frac{1-\bar{a}^u_j}{\bar{a}^u_j}\right)^{\zeta}\right)} \right) \right)^{1/\zeta} \right) \right), 1-\left(\frac{1}{\left(\left(1+\left(\frac{\mathfrak{Y}\left(\mathfrak{Y}-1\right)}{2}\right)^{1/\zeta} \times 1/\left(\sum_{\substack{\mathrm{i},j=1\\ \mathrm{i}\neq j}}^{\mathfrak{Y}} \frac{1}{\left(\left(\frac{\mathfrak{z}^l_{\mathrm{i}}}{1-\mathfrak{z}^l_1}\right)^{\zeta}+\left(\frac{\mathfrak{z}^l_j}{1-\mathfrak{z}^l_j}\right)^{\zeta}\right)} \right) \right)^{1/\zeta} \right)}, \left(1+\left(\frac{\mathfrak{Y}\left(\mathfrak{Y}-1\right)}{2}\right)^{1/\zeta} \times 1/\left(\sum_{\substack{\mathrm{i},j=1\\ \mathrm{i}\neq j}}^{\mathfrak{Y}} \frac{1}{\left(\left(\frac{\mathfrak{z}^u_{\mathrm{i}}}{1-\mathfrak{z}^u_1}\right)^{\zeta}+\left(\frac{\mathfrak{z}^u_j}{1-\mathfrak{z}^u_j}\right)^{\zeta}\right)} \right) \right)^{1/\zeta} \right)$$

and weights, which may bring subjectivity unless automated or optimized methods are used. Subsequent research could alleviate these by investigating lightweight solutions, hybrid parameter tuning optimization algorithms, and automatic criteria selection to minimize the need for expert input.

$$IVIFDGBM^{\mathfrak{s},0}\left(\varrho_1,\varrho_2,\ldots,\varrho_{\mathfrak{Y}}\right)$$

$$= \lim_{\mathfrak{b}\to 0}\left[1 - 1\Big/\left(\left(1+\left(\frac{\mathfrak{Y}(\mathfrak{Y}-1)}{\mathfrak{s}+\mathfrak{b}} \times \frac{1}{\left(\sum_{\substack{\mathsf{i},j=1\\ \mathsf{i}\neq j}}^{\mathfrak{Y}} \frac{1}{\left(\mathfrak{s}\left(\frac{\bar{a}^{l}_{\mathsf{i}}}{1-\bar{a}^{l}_{\mathsf{i}}}\right)^{\zeta} + \mathfrak{b}\left(\frac{\bar{a}^{l}_{j}}{1-\bar{a}^{l}_{j}}\right)^{\zeta}\right)}\right)}\right)^{1/\zeta}\right), \left(\frac{\mathfrak{Y}(\mathfrak{Y}-1)}{\mathfrak{s}+\mathfrak{b}} \times \frac{1}{\left(\sum_{\substack{\mathsf{i},j=1\\ \mathsf{i}\neq j}}^{\mathfrak{Y}} \frac{1}{\left(\mathfrak{s}\left(\frac{\bar{a}^{u}_{\mathsf{i}}}{1-\bar{a}^{u}_{\mathsf{i}}}\right)^{\zeta} + \mathfrak{b}\left(\frac{\bar{a}^{u}_{j}}{1-\bar{a}^{u}_{j}}\right)^{\zeta}\right)}\right)}\right)^{1/\zeta}\right)\right],$$

$$\left(\frac{1}{\left(\left(1+\left(\frac{\mathfrak{Y}(\mathfrak{Y}-1)}{\mathfrak{s}+\mathfrak{b}} \times 1\Big/\left(\sum_{\substack{\mathsf{i},j=1\\ \mathsf{i}\neq j}}^{\mathfrak{Y}} \frac{1}{\left(\mathfrak{s}\left(\frac{1-\mathfrak{z}^{l}_{\mathsf{i}}}{\mathfrak{z}^{l}_{1}}\right)^{\zeta} + \mathfrak{b}\left(\frac{1-\mathfrak{z}^{l}_{j}}{\mathfrak{z}^{l}_{j}}\right)^{\zeta}\right)}\right)\right)^{1/\zeta}\right), \left(\frac{\mathfrak{Y}(\mathfrak{Y}-1)}{\mathfrak{s}+\mathfrak{b}} \times 1\Big/\left(\sum_{\substack{\mathsf{i},j=1\\ \mathsf{i}\neq j}}^{\mathfrak{Y}} \frac{1}{\left(\mathfrak{s}\left(\frac{1-\mathfrak{z}^{u}_{\mathsf{i}}}{\mathfrak{z}^{u}_{1}}\right)^{\zeta} + \mathfrak{b}\left(\frac{1-\mathfrak{z}^{u}_{j}}{\mathfrak{z}^{u}_{j}}\right)^{\zeta}\right)}\right)\right)^{1/\zeta}\right)}\right)$$

IX. CONCLUSION

This study presents a novel approach applying artificial intelligence and deep learning to enhance smart sensor networks and carbon-based biosensors for optoelectronic device innovation. By integrating AI-driven methodologies, the proposed framework effectively addresses the complexities and uncertainties associated with real-time environmental monitoring and healthcare diagnostics. The deep learning approach enables precise data processing, pattern recognition, and predictive analytics, optimizing the performance and efficiency of smart sensor networks.

Theoretical aspects of deep learning-based sensor networks are outlined, and their practical applicability is demonstrated through a structured numerical analysis. The evaluation, conducted using four AI-driven alternatives and multiple criteria, highlights the superiority of hybrid deep learning models in terms of accuracy, robustness, computational efficiency, and energy consumption. Comparative analysis with traditional models further emphasizes the benefits of AI-powered solutions in enhancing the effectiveness of biosensors and optoelectronic systems. The findings underscore the potential of AI-driven deep learning techniques as a transformative tool in advancing smart sensor networks and biosensor technology. By leveraging deep learning algorithms, researchers and industry professionals can significantly enhance detection capabilities, improve real-time decision-making, and optimize energy efficiency in optoelectronic applications. This study contributes to the growing body of knowledge in AI-driven sensor innovation and establishes a foundation for future research on expanding AI's role in intelligent sensing, predictive modeling, and real-time adaptive decision-making.

$$
= \left(1 - 1\Big/ \left(\begin{array}{c} 1 + \left(\begin{array}{c} \left(\frac{\mathfrak{Y}(\mathfrak{Y}-1)}{\mathfrak{s}}\right)^{1/\zeta} \\ \times 1\Big/ \left(\sum_{\substack{\mathrm{i},j=1 \\ \mathrm{i}\neq j}}^{\mathfrak{Y}} \frac{1}{\left(\mathfrak{s}\left(\frac{\bar{a}_{\mathrm{i}}^{l}}{1-\bar{a}_{\mathrm{i}}^{l}}\right)\right)^{\zeta}} \right) \end{array} \right)^{1/\zeta} , \\ \left(\begin{array}{c} \left(\frac{\mathfrak{Y}(\mathfrak{Y}-1)}{\mathfrak{s}}\right)^{1/\zeta} \\ \times 1\Big/ \left(\sum_{\substack{\mathrm{i},j=1 \\ \mathrm{i}\neq j}}^{\mathfrak{Y}} \frac{1}{\left(\mathfrak{s}\left(\frac{\bar{a}_{\mathrm{i}}^{u}}{1-\bar{a}_{\mathrm{i}}^{u}}\right)\right)^{\zeta}} \right) \end{array} \right)^{1/\zeta} \end{array} \right) \right), \left(\begin{array}{c} 1/1 + \left(\left(\frac{\mathfrak{Y}(\mathfrak{Y}-1)}{\mathfrak{s}}\right)^{1/\zeta} \times 1\Big/ \left(\sum_{\mathrm{i}=1}^{\mathfrak{Y}} \frac{1}{\left(\mathfrak{s}\left(\frac{1-\mathfrak{z}_{\mathrm{i}}^{l}}{\mathfrak{z}_{1}^{l}}\right)\right)^{\zeta}} \right) \right)^{1/\zeta} \\ \left(\left(\frac{\mathfrak{Y}(\mathfrak{Y}-1)}{\mathfrak{s}}\right)^{1/\zeta} \times 1\Big/ \left(\sum_{\mathrm{i}=1}^{\mathfrak{Y}} \frac{1}{\left(\mathfrak{s}\left(\frac{1-\mathfrak{z}_{\mathrm{i}}^{u}}{\mathfrak{z}_{1}^{u}}\right)\right)^{\zeta}} \right) \right)^{1/\zeta} \end{array} \right)
$$

$$
IVIFDGBM^{1,0}\left(\varrho_1, \varrho_2, \ldots, \varrho_{\mathfrak{Y}}\right)
$$

$$
= \left(1 - 1\Big/ \left(\begin{array}{c} 1 + \left(\begin{array}{c} \left(\mathfrak{Y}(\mathfrak{Y}-1)\right)^{1/\zeta} \\ \Big/ \left(\sum_{\mathrm{i}=1}^{\mathfrak{Y}} \frac{1}{\left(\left(\frac{\bar{a}_{\mathrm{i}}^{l}}{1-\bar{a}_{\mathrm{i}}^{l}}\right)\right)^{\zeta}} \right) \end{array} \right)^{1/\zeta} , \\ 1 + \left(\begin{array}{c} \left(\mathfrak{Y}(\mathfrak{Y}-1)\right)^{1/\zeta} \\ \Big/ \left(\sum_{\mathrm{i}=1}^{\mathfrak{Y}} \frac{1}{\left(\left(\frac{\bar{a}_{\mathrm{i}}^{u}}{1-\bar{a}_{\mathrm{i}}^{u}}\right)\right)^{\zeta}} \right) \end{array} \right)^{1/\zeta} \end{array} \right) \right) 1 - \left(\frac{1}{\left(\begin{array}{c} 1 + \left(\left(\mathfrak{Y}(\mathfrak{Y}-1)\right)^{1/\zeta} \Big/ \left(\sum_{\mathrm{i}=1}^{\mathfrak{Y}} \frac{1}{\left(\left(\frac{1-\mathfrak{z}_{\mathrm{i}}^{l}}{\mathfrak{z}_{1}^{l}}\right)\right)^{\zeta}} \right) \right)^{1/\zeta} , \\ \left(\left(\mathfrak{Y}(\mathfrak{Y}-1)\right)^{1/\zeta} \Big/ \left(\sum_{\mathrm{i}=1}^{\mathfrak{Y}} \frac{1}{\left(\left(\frac{1-\mathfrak{z}_{\mathrm{i}}^{u}}{\mathfrak{z}_{1}^{u}}\right)\right)^{\zeta}} \right) \right)^{1/\zeta} \end{array} \right)} \right)
$$

APPENDIX A
PROOF OF APPENDIX A

The particular instances of the $IVIFDBM^{\text{ß},\text{ƀ}}$ operator for the parameters ß and ƀ will be examined in the following.

1) When $\text{ƀ} \to 0,\ \zeta > 0,$ then we can get, as shown in the equation at the bottom of page 20.
2) When $\text{ß} = 1,\ \text{ƀ} \to 0,\ \zeta > 0,$ then we can get, as shown in the equation at the bottom of page 21.

$$IVIFDGBM^{0,\text{ƀ}}\left(\varrho_1, \varrho_2, \ldots, \varrho_{\mathfrak{Y}}\right) = \left(1 - 1/\left(\frac{\left(1+\left(\frac{\mathfrak{Y}(\mathfrak{Y}-1)}{\text{ƀ}}\right)^{1/\zeta} \times 1/\left(\sum_{\substack{\mathsf{i},j=1\\ \mathsf{i}\neq j}}^{\mathfrak{Y}} \frac{1}{\left(\text{ƀ}\left(\frac{\bar{a}_j^l}{1-\bar{a}_j^l}\right)^{\zeta}\right)}\right)\right)^{1/\zeta}}{\left(1+\left(\frac{\mathfrak{Y}(\mathfrak{Y}-1)}{\text{ƀ}}\right)^{1/\zeta} \times 1/\left(\sum_{\substack{\mathsf{i},j=1\\ \mathsf{i}\neq j}}^{\mathfrak{Y}} \frac{1}{\left(\text{ƀ}\left(\frac{\bar{a}_j^u}{1-\bar{a}_j^u}\right)^{\zeta}\right)}\right)\right)^{1/\zeta}} \right), 1 - \left(\frac{\dfrac{1}{\left(\left(1+\left(\frac{\mathfrak{Y}(\mathfrak{Y}-1)}{\text{ƀ}}\right)^{1/\zeta} \times 1/\left(\sum_{\substack{\mathsf{i},j=1\\ \mathsf{i}\neq j}}^{\mathfrak{Y}} \frac{1}{\left(\text{ƀ}\left(\frac{1-\text{ʒ}_j^l}{\text{ʒ}_j^l}\right)^{\zeta}\right)}\right)\right)^{1/\zeta}\right)},}{\left(1+\left(\frac{\mathfrak{Y}(\mathfrak{Y}-1)}{\text{ƀ}}\right)^{1/\zeta} \times 1/\left(\sum_{\substack{\mathsf{i},j=1\\ \mathsf{i}\neq j}}^{\mathfrak{Y}} \frac{1}{\left(\text{ƀ}\left(\frac{1-\text{ʒ}_j^u}{\text{ʒ}_j^u}\right)^{\zeta}\right)}\right)\right)^{1/\zeta}} \right) \right)$$

$$IVIFDGBM^{1,1}\left(\varrho_1, \varrho_2, \ldots, \varrho_{\mathfrak{Y}}\right) = \left(1 - 1/\left(\frac{\left(1+\left(\frac{\mathfrak{Y}(\mathfrak{Y}-1)}{2}\right)^{1/\zeta} \times 1/\left(\sum_{\substack{\mathsf{i},j=1\\ \mathsf{i}\neq j}}^{\mathfrak{Y}} \frac{1}{\left(\left(\frac{\bar{a}_{\mathsf{i}}^l}{1-\bar{a}_{\mathsf{i}}^l}\right)^{\zeta} + \left(\frac{\bar{a}_j^l}{1-\bar{a}_j^l}\right)^{\zeta}\right)}\right)\right)^{1/\zeta}}{\left(1+\left(\frac{\mathfrak{Y}(\mathfrak{Y}-1)}{2}\right)^{1/\zeta} \times 1/\left(\sum_{\substack{\mathsf{i},j=1\\ \mathsf{i}\neq j}}^{\mathfrak{Y}} \frac{1}{\left(\left(\frac{\bar{a}_{\mathsf{i}}^u}{1-\bar{a}_{\mathsf{i}}^u}\right)^{\zeta} + \left(\frac{\bar{a}_j^u}{1-\bar{a}_j^u}\right)^{\zeta}\right)}\right)\right)^{1/\zeta}} \right), 1 - \left(\frac{\dfrac{1}{\left(\left(1+\left(\frac{\mathfrak{Y}(\mathfrak{Y}-1)}{2}\right)^{1/\zeta} \times 1/\left(\sum_{\substack{\mathsf{i},j=1\\ \mathsf{i}\neq j}}^{\mathfrak{Y}} \frac{1}{\left(\left(\frac{1-\text{ʒ}_{\mathsf{i}}^l}{\text{ʒ}_1^l}\right)^{\zeta} + \left(\frac{1-\text{ʒ}_j^l}{\text{ʒ}_j^l}\right)^{\zeta}\right)}\right)\right)^{1/\zeta}\right)},}{\left(1+\left(\frac{\mathfrak{Y}(\mathfrak{Y}-1)}{2}\right)^{1/\zeta} \times 1/\left(\sum_{\substack{\mathsf{i},j=1\\ \mathsf{i}\neq j}}^{\mathfrak{Y}} \frac{1}{\left(\left(\frac{1-\text{ʒ}_{\mathsf{i}}^u}{\text{ʒ}_1^u}\right)^{\zeta} + \left(\frac{1-\text{ʒ}_j^u}{\text{ʒ}_j^u}\right)^{\zeta}\right)}\right)\right)^{1/\zeta}} \right) \right)$$

3) When $ꞩ \to 0,\ \zeta > 0,$ then we can get, as shown in the equation at the bottom of page 21.
4) When $ꞩ = ƀ = 1,\ \zeta > 0,$ then we can get, as shown in the equation at the bottom of page 22.

The interrelationships between the input parameters can be considered by the IVIFDBM operator, but the parameters are not self-important. The importance of parameters in MADM or MAGDM situations is comparable to attribute weights or expert weights. The IFDBM operator has a flaw, which we shall address by defining an interval-valued intuitionistic fuzzy weighted Dombi Bonferroni mean operator.

APPENDIX B
PROOF OF APPENDIX B

The proof, identical to Proposition 4's, is not included here.

In the following, we will study some exceptional cases of the *IVIFDGBM*^{ꞩ,ƀ} operator regarding the parameters $ꞩ$ and $ƀ$.

1) When $ƀ \to 0,\ \zeta > 0,$ then we can get, as shown in the equation at the bottom of pages 23 and 24.

When $ꞩ = 1,\ ƀ \to 0,\ \zeta > 0,$ then we can get, as shown in the equation at the bottom of page 24.

When $ꞩ \to 0,\ \zeta > 0,$ then we can get, as shown in the equation at the bottom of page 25.

When $ꞩ = ƀ = 1,\ \zeta > 0,$ then we can get, as shown in the equation at the bottom of page 24.

In a similar way, the *IVIFWDGBM*^{ꞩ,ƀ} operator does not account for the significance of individual input parameters; instead, it just considers the input parameters and their interactions. To address these two points in detail, we will define an interval-valued intuitionistic fuzzy weighted Dombi geometric Bonferroni mean (IVIFWDGBM) operator.

REFERENCES

[1] L. A. Zadeh, "Fuzzy sets," *Inf. Control*, vol. 8, no. 3, pp. 338–353, Jun. 1965, doi: 10.1016/s0019-9958(65)90241-x.

[2] K. T. Atanassov, "Intuitionistic fuzzy sets," *Fuzzy Sets Syst.*, vol. 20, no. 1, pp. 87–96, Aug. 1986, doi: 10.1016/s0165-0114(86)80034-3.

[3] K. Atanassov and G. Gargov, "Interval valued intuitionistic fuzzy sets," *Fuzzy Sets Syst.*, vol. 31, no. 3, pp. 343–349, Jul. 1989, doi: 10.1016/0165-0114(89)90205-4.

[4] S. Ali, A. Ali, A. B. Azim, A. ALoqaily, and N. Mlaiki, "Averaging aggregation operators under the environment of q-rung orthopair picture fuzzy soft sets and their applications in MADM problems," *AIMS Math.*, vol. 8, no. 4, pp. 9027–9053, 2023.

[5] M. Akram, K. Ullah, and D. Pamucar, "Performance evaluation of solar energy cells using the interval-valued T-Spherical fuzzy Bonferroni mean operators," *Energies*, vol. 15, no. 1, p. 292, Jan. 2022.

[6] T. Mahmood, K. Ullah, Q. Khan, and N. Jan, "An approach toward decision-making and medical diagnosis problems using the concept of spherical fuzzy sets," *Neural Comput. Appl.*, vol. 31, no. 11, pp. 7041–7053, Nov. 2019, doi: 10.1007/s00521-018-3521-2.

[7] K. Ullah, N. Hassan, T. Mahmood, N. Jan, and M. Hassan, "Evaluation of investment policy based on multi-attribute decision-making using interval valued T-Spherical fuzzy aggregation operators," *Symmetry*, vol. 11, no. 3, p. 357, Mar. 2019.

[8] Z. Sabir, M. Umar, S. Salahshour, and T. Saeed, "A reliable neural network procedure for the novel sixth-order nonlinear singular pantograph differential model," *Mod. Phys. Lett. B*, vol. 39, no. 12, Apr. 2025, Art. no. 2450473.

[9] Z. Sabir, S. Khansa, G. Baltaji, and T. Saeed, "A Bayesian regularization neural network procedure to solve the language learning system," *Knowl.-Based Syst.*, vol. 310, Feb. 2025, Art. no. 112997.

[10] Z. Sabir, I. A. Kotob, L. A. Sheikh, and T. Saeed, "A novel computational approach-based hyperbolic tangent sigmoid deep neural network for the hepatitis b virus model," *Int. J. Geometric Methods Mod. Phys.*, vol. 22, no. 4, Mar. 2025, Art. no. 2450315, doi: 10.1142/s0219887824503158.

[11] M. Umar, Z. Sabir, M. A. Z. Raja, F. Amin, T. Saeed, and Y. G. Sanchez, "Design of intelligent computing solver with Morlet wavelet neural networks for nonlinear predator–prey model," *Appl. Soft Comput.*, vol. 134, Feb. 2023, Art. no. 109975, doi: 10.1016/j.asoc.2022.109975.

[12] S. A. Bhat, Z. Sabir, M. A. Z. Raja, T. Saeed, and A. M. Alshehri, "A novel heuristic Morlet wavelet neural network procedure to solve the delay differential perturbed singular model," *Knowl.-Based Syst.*, vol. 2, Apr. 2024, Art. no. 111624.

[13] Z. Sabir, T. Saeed, J. L. G. Guirao, J. M. Sánchez, and A. Valverde, "A swarming Meyer wavelet computing approach to solve the transport system of goods," *Axioms*, vol. 12, no. 5, p. 456, May 2023.

[14] T. Saeed, J. L. G. Guirao, Z. Sabir, H. H. Alsulami, and Y. G. Sánchez, "A computational approach to solve the nonlinear biological prey–predator system," *Fractals*, vol. 30, no. 10, Dec. 2022, Art. no. 2240267, doi: 10.1142/s0218348x22402678.

[15] Z. Sabir, M. A. Zahoor Raja, J. L. G. Guirao, and T. Saeed, "Design of Mayer wavelet neural networks for solving functional nonlinear singular differential equation," *Math. Problems Eng.*, vol. 2022, pp. 1–11, Apr. 2022, doi: 10.1155/2022/1213370.

[16] T. Saeed, Z. Sabir, M. Sh. Alhodaly, H. H. Alsulami, and Y. Guerrero Sánchez, "An advanced heuristic approach for a nonlinear mathematical based medical smoking model," *Results Phys.*, vol. 32, Jan. 2022, Art. no. 105137.

[17] Z. Sabir, M. A. Z. Raja, J. L. G. Guirao, and T. Saeed, "Meyer wavelet neural networks to solve a novel design of fractional order pantograph lane-emden differential model," *Chaos, Solitons Fractals*, vol. 152, Nov. 2021, Art. no. 111404.

[18] Z. Sabir, M. A. Z. Raja, J. L. Guirao, and T. Saeed, "Meyer wavelet neural networks to solve a novel design of fractional order pantograph Lane–Emden differential model," *Chaos Solitons Fractals*, vol. 9, Apr. 2021, Art. no. 111404.

[19] M. Umar, Z. Sabir, M. A. Z. Raja, F. Amin, T. Saeed, and Y. Guerrero-Sanchez, "Integrated neuro-swarm heuristic with interior-point for nonlinear SITR model for dynamics of novel COVID-19," *Alex. Eng. J.*, vol. 1, no. 3, pp. 2811–2824, 2021.

[20] Z. Sabir, J. L. G. Guirao, T. Saeed, and F. Erdoğan, "Design of a novel second-order prediction differential model solved by using Adams and explicit Runge–Kutta numerical methods," *Math. Problems Eng.*, vol. 2020, pp. 1–7, Jul. 2020, doi: 10.1155/2020/9704968.

[21] J. L. G. Guirao, Z. Sabir, and T. Saeed, "Design and numerical solutions of a novel third-order nonlinear Emden–Fowler delay differential model," *Math. Problems Eng.*, vol. 2020, pp. 1–9, Aug. 2020, doi: 10.1155/2020/7359242.

[22] M. A. Abdelkawy, Z. Sabir, J. L. G. Guirao, and T. Saeed, "Numerical investigations of a new singular second-order nonlinear coupled functional Lane–Emden model," *Open Phys.*, vol. 18, no. 1, pp. 770–778, Nov. 2020, doi: 10.1515/phys-2020-0185.

[23] Z. Sabir, J. L. G. Guirao, and T. Saeed, "Solving a novel designed second order nonlinear Lane–Emden delay differential model using the heuristic techniques," *Chaos Solitons Fractals*, vol. 102, Jan. 2021, Art. no. 107105.

[24] Z. Sabir, M. A. Z. Raja, A. Kamal, J. L. G. Guirao, D.-N. Le, T. Saeed, and M. Salama, "Neuro-swarm heuristic using interior-point algorithm to solve a third kind of multi-singular nonlinear system," *Math. Biosci. Eng.*, vol. 18, no. 5, pp. 5285–5308, 2021.

[25] S. Hussain, A. Zeb, A. Rasheed, and T. Saeed, "Stochastic mathematical model for the spread and control of corona virus," *Adv. Difference Equ.*, vol. 2020, no. 1, p. 574, Dec. 2020, doi: 10.1186/s13662-020-03029-6.

[26] R. R. Yager and J. Kacprzyk, *The Ordered Weighted Averaging Operators: Theory and Applications*. Cham, Switzerland: Springer, 2012.

[27] T. Calvo, G. Mayor, and R. Mesiar, *Aggregation Operators: New Trends and Applications*, vol. 97. Cham, Switzerland: Springer, 2002.

[28] Z. S. Xu and Q. L. Da, "An overview of operators for aggregating information," *Int. J. Intell. Syst.*, vol. 18, no. 9, pp. 953–969, Sep. 2003, doi: 10.1002/int.10127.

[29] V. Torra and Y. Narukawa, *Modeling Decisions: Information Fusion and Aggregation Operators*. Cham, Switzerland: Springer, 2007.

[30] R. R. Yager, "The power average operator," *IEEE Trans. Syst., Man, Cybern., A, Syst. Humans*, vol. 31, no. 6, pp. 724–731, Nov. 2001, doi: 10.1109/3468.983429.
[31] P. Liu and X. Yu, "Density aggregation operators based on the intuitionistic trapezoidal fuzzy numbers for multiple attribute decision making," *Technol. Econ. Develop. Economy*, vol. 19, pp. S454–S470, Jan. 2014, doi: 10.3846/20294913.2013.881436.
[32] C. Bonferroni, "Sulle medie multiple di potenze," *Boll. DellUnione Mat. Ital.*, vol. 5, pp. 267–270, Jan. 1950.
[33] R. R. Yager, "On generalized Bonferroni mean operators for multi-criteria aggregation," *Int. J. Approx. Reasoning*, vol. 50, no. 8, pp. 1279–1286, Sep. 2009.
[34] S. Sýkora, "Mathematical means and averages: Generalized Heronian means," Stan's Library, Castano Primo, Italy, Tech. Rep., 2009.
[35] Z. Xu and R. R. Yager, "Intuitionistic fuzzy Bonferroni means," *IEEE Trans. Syst., Man, Cybern., B Cybern.*, vol. 41, no. 2, pp. 568–578, Apr. 2011, doi: 10.1109/TSMCB.2010.2072918.
[36] M. Xia, Z. Xu, and B. Zhu, "Geometric Bonferroni means with their application in multi-criteria decision making," *Knowl.-Based Syst.*, vol. 40, pp. 88–100, Mar. 2013, doi: 10.1016/j.knosys.2012.11.013.
[37] D. Li, W. Zeng, and J. Li, "Geometric Bonferroni mean operators," *Int. J. Intell. Syst.*, vol. 31, no. 12, pp. 1181–1197, Dec. 2016, doi: 10.1002/int.21822.
[38] B. Zhu and Z. S. Xu, "Hesitant fuzzy Bonferroni means for multi-criteria decision making," *J. Oper. Res. Soc.*, vol. 64, no. 12, pp. 1831–1840, Dec. 2013, doi: 10.1057/jors.2013.7.
[39] B. Zhu, Z. Xu, and M. Xia, "Hesitant fuzzy geometric Bonferroni means," *Inf. Sci.*, vol. 205, pp. 72–85, Nov. 2012, doi: 10.1016/j.ins.2012.01.048.
[40] Y. He, Z. He, C. Jin, and H. Chen, "Intuitionistic fuzzy power geometric Bonferroni means and their application to multiple attribute group decision making," *Int. J. Uncertainty, Fuzziness Knowl.-Based Syst.*, vol. 23, no. 2, pp. 285–315, Apr. 2015.
[41] G. Wei, X. Zhao, R. Lin, and H. Wang, "Uncertain linguistic Bonferroni mean operators and their application to multiple attribute decision making," *Appl. Math. Model.*, vol. 37, no. 7, pp. 5277–5285, Apr. 2013.
[42] Z. Liu and P. Liu, "Intuitionistic uncertain linguistic partitioned Bonferroni means and their application to multiple attribute decision-making," *Int. J. Syst. Sci.*, vol. 4, no. 5, pp. 1092–1105, 2017.
[43] J. Dombi, "A general class of fuzzy operators, the demorgan class of fuzzy operators and fuzziness measures induced by fuzzy operators," *Fuzzy Sets Syst.*, vol. 8, no. 2, pp. 149–163, Aug. 1982.
[44] S. Abdullah, M. Aslam, and K. Ullah, "Bipolar fuzzy soft sets and its applications in decision making problem," *J. Intell. Fuzzy Syst.*, vol. 27, no. 2, pp. 729–742, Aug. 2014.
[45] T. Mahmood and U. U. Rehman, "A method to multi-attribute decision making technique based on dombi aggregation operators under bipolar complex fuzzy information," *Comput. Appl. Math.*, vol. 41, no. 1, p. 47, Jan. 2022, doi: 10.1007/s40314-021-01735-9.
[46] M. R. Seikh and U. Mandal, "Intuitionistic fuzzy dombi aggregation operators and their application to multiple attribute decision-making," *Granular Comput.*, vol. 6, no. 3, pp. 473–488, Jul. 2021, doi: 10.1007/s41066-019-00209-y.
[47] K. T. Atanassov, "Interval Valued Intuitionistic Fuzzy Sets," in *Intuitionistic Fuzzy Sets: Theory and Applications* (Studies in Fuzziness and Soft Computing), K. T. Atanassov, Ed., Heidelberg, Germany: Physica-Verlag HD, 1999, pp. 139–177, doi: 10.1007/978-3-7908-1870-3_2.
[48] L. Wu, G. Wei, H. Gao, and Y. Wei, "Some interval-valued intuitionistic fuzzy dombi Hamy mean operators and their application for evaluating the elderly tourism service quality in tourism destination," *Mathematics*, vol. 6, no. 12, p. 294, Dec. 2018, doi: 10.3390/math6120294.
[49] T. Senapati, G. Chen, R. Mesiar, and R. R. Yager, "Novel Aczel–Alsina operations-based interval-valued intuitionistic fuzzy aggregation operators and their applications in multiple attribute decision-making process," *Int. J. Intell. Syst.*, vol. 37, no. 8, pp. 5059–5081, Aug. 2022, doi: 10.1002/int.22751.

KELIANG LUO received the bachelor's degree in computer and electronic engineering from the School of Science and Technology, Hong Kong Metropolitan University, in 2022. He is currently pursuing the master's degree in software engineering with the Faculty of Computer Science and Information Technology, Universiti Putra Malaysia. His research areas and directions include reinforcement learning and carbon-based biosensors.